~~SECURITY INFORMATION~~

[redacted]

Copy 5
RM L52E23

AUG 13 1952

NACA RM L52E23

CLASSIFICATION CHANGED

UNCLASSIFIED

To ________ By authority of NACA Res abs #RN-127 Date effective May 16 1958 AMT 6-13-58

RESEARCH MEMORANDUM

AERODYNAMIC CHARACTERISTICS AT SUPERSONIC SPEEDS OF A SERIES OF WING-BODY COMBINATIONS HAVING CAMBERED WINGS WITH AN ASPECT RATIO OF 3.5 AND A TAPER RATIO OF 0.2

EFFECTS OF SWEEP ANGLE AND THICKNESS RATIO ON THE STATIC LATERAL STABILITY CHARACTERISTICS AT $M =$

FOR REFERENCE

NOT TO BE TAKEN FROM THIS ROOM

By Clyde V. Hamilton

Langley Aeronautical Laboratory
Langley Field, Va.

NATIONAL ADVISORY COMMITTEE FOR AERONAUTICS

WASHINGTON

August 1, 1952

[redacted]

NATIONAL ADVISORY COMMITTEE FOR AERONAUTICS

RESEARCH MEMORANDUM

AERODYNAMIC CHARACTERISTICS AT SUPERSONIC SPEEDS OF A SERIES OF WING-BODY COMBINATIONS HAVING CAMBERED WINGS WITH AN ASPECT RATIO OF 3.5 AND A TAPER RATIO OF 0.2

EFFECTS OF SWEEP ANGLE AND THICKNESS RATIO ON THE STATIC LATERAL STABILITY CHARACTERISTICS AT $M = 2.01$

By Clyde V. Hamilton

SUMMARY

An investigation has been conducted in the Langley 4- by 4-foot supersonic pressure tunnel at a Mach number of 2.01 and a Reynolds number of 2.2×10^6 to determine the effects of sweep angle and thickness ratio on the static lateral stability characteristics of a series of wings having a taper ratio of 0.2 and an aspect ratio of 3.5. The wings, which were tested on a body of revolution, had sweep angles of 10.8°, 35°, and 47° for a thickness ratio of 4 percent and thickness ratios of 4, 6, and 9 percent for a sweep angle of 47°. In addition, the wing with a thickness ratio of 6 percent and a sweep angle of 47° was tested with and without nacelles installed.

The results of these tests indicate that at a Mach number of 2.01 both the lateral-force parameter C_{Y_ψ} and the directional-stability parameter C_{n_ψ} tend to increase with lift coefficient. The effect of increasing the sweep angle or thickness ratio is to increase the positive value of C_{Y_ψ} and decrease the positive value of C_{n_ψ}. The effect of nacelle installation is to increase the positive values of C_{Y_ψ} and C_{n_ψ} and the negative value of C_{l_ψ}.

[redacted]

A change in Mach number from 1.60 to 2.01 had little effect on $C_{Y_{\psi}}$ but increased the positive values of $C_{n_{\psi}}$.

INTRODUCTION

A research program has been in progress at the Langley Aeronautical Laboratory to determine at subsonic, transonic, and supersonic speeds, the effects of thickness and sweep on the aerodynamic characteristics of a series of wing-body combinations with cambered wings having a taper ratio of 0.2 and an aspect ratio of 3.5. The effects of thickness and sweep on the longitudinal characteristics of a series of wing-body combinations at subsonic and transonic speeds are presented in references 1 and 2, respectively. The effects of sweep and thickness on the longitudinal characteristics for the series of wing-body combinations at Mach numbers of 1.60 and 2.01 are presented in references 3 and 4, respectively. The results of tests of several nacelle installations on a 47° sweptback wing at Mach numbers of 1.60 and 2.01 are presented in references 5 and 6, respectively. The effects of sweep and thickness on the lateral characteristics for the series of wing-body combinations at a Mach number of 1.60 are presented in reference 7.

The present paper presents the results of tests of the same series of wing-body combinations reported in reference 7 at a Mach number of 2.01 and a Reynolds number of 2.2×10^6 based on the wing mean aerodynamic chord. For the sweep series, the wings had quarter-chord sweep angles of 10.8°, 35°, and 47° with a thickness ratio of 4 percent and for the thickness series, thickness ratios of 4, 6, and 9 percent with a sweep angle of 47°. In addition, a wing of 47° sweep with thickened root sections was tested. For this wing, the thickness ratio tapered linearly from 12 percent at the root to 6 percent at the 40-percent-semispan station and was constant at 6 percent farther outboard. The effects of adding nacelles to the 6-percent-thick wing were also investigated. The results are presented with a minimum of analysis to expedite publication.

COEFFICIENTS AND SYMBOLS

The results of the tests are presented as standard NACA coefficients of forces and moments. The data are referred to the stability-axis system (fig. 1) with the reference center of gravity at 25 percent of the wing mean aerodynamic chord.

The coefficients and symbols are defined as follows:

C_Y	lateral-force coefficient, Y/qS
C_n	yawing-moment coefficient, N/qSb
C_l	rolling-moment coefficient, L/qSb
C_L	lift coefficient, $\frac{-Z}{qS}$
C_X	longitudinal-force coefficient, X/qS
C_m	pitching-moment coefficient, $M'/qS\bar{c}$
X	force along X-axis
Y	force along Y-axis
Z	force along Z-axis
L	moment about X-axis
M'	moment about Y-axis
N	moment about Z-axis
q	free-stream dynamic pressure
S	total wing area
b	wing span
$\bar{c}$	wing mean aerodynamic chord
M	Mach number
t/c	thickness ratio, Wing thickness/Wing chord
α	angle of attack of body center line, deg
ψ	angle of yaw, deg
Λ	angle of sweep of wing quarter-chord line, deg
C_{Y_ψ}	lateral-force parameter, rate of change of lateral-force coefficient with angle of yaw, $\delta C_Y/\delta\psi$

C_{n_ψ} directional-stability parameter, rate of change of yawing-moment coefficient with angle of yaw, $\delta C_n/\delta\psi$

C_{l_ψ} effective-dihedral parameter, rate of change of rolling-moment coefficient with angle of yaw, $\delta C_l/\delta\psi$

APPARATUS AND MODELS

Tunnel

The tests were conducted in the Langley 4- by 4-foot supersonic pressure tunnel which is described in reference 7.

Models

The models used in these tests were composed of an ogive-cylinder body and various midwing configurations with a ratio of body diameter to wing span of about 0.094. The wings were positioned so that the quarter-chord point of the mean aerodynamic chord was always at the same body station. The wing airfoil sections had an NACA 65A-series thickness distribution with mean-line ordinates one-third of the NACA 230 series plus an $(a = 1)$ mean line for $C_L = 0.1$. The airfoil coordinates are given in table I. Details of the models are shown in figure 2.

The models were sting-supported and had a six-component internal strain-gage balance in the body. The model and sting are shown in figure 3.

TESTS

Test Conditions

The conditions for the tests were:

Mach number	2.01
Reynolds number, based on wing mean aerodynamic chord . . .	2.2×10^6
Stagnation dew point, °F	<-30
Stagnation pressure, lb/sq in.	14
Stagnation temperature, °F	110

A limited calibration prior to these tests has shown that the flow in the test section is reasonably uniform. The magnitudes of the variations in the flow parameters are summarized in the following table:

Mach number	± 0.01
Flow angle in horizontal plane, deg	± 0.1
Flow angle in vertical plane, deg	± 0.1

Test Procedure

The tests were made through an angle-of-yaw range from -4° to 8° at an angle of attack of 0° and 5.3° and through an angle-of-attack range from -2° to 13° at $\psi = 0^{\circ}$ and 5°.

Corrections and Accuracy

The angles of attack and yaw were corrected for the deflection of the balance under load. The angle corrections were determined from an in-place calibration of the balance for various lift loads, pitching moments, side loads, and yawing moments. The estimated accuracy of both the angle-of-attack and angle-of-yaw settings was $\pm 0.10^{\circ}$. No corrections were applied to the data to account for flow variations in the test section.

The estimated errors in the force data obtained by comparing the results of two tests of the same configuration are as follows:

C_L	± 0.001
C_D	± 0.001
C_m	± 0.001
C_Y	± 0.002
C_n	± 0.0002
C_l	± 0.0002

The base pressure was measured and the drag data were corrected to correspond to a base pressure equal to the free-stream static pressure.

RESULTS

The results are presented in this paper with a minimum of analysis to expedite publication. The aerodynamic characteristics in yaw for various configurations at $\alpha = 0^{\circ}$ and $\alpha = 5.3^{\circ}$ are presented in figure 4. The effects of yaw on the lateral characteristics in pitch for

various configurations are shown in figure 5. The variation of the static lateral-stability characteristics with lift coefficient for various configurations is presented in figure 6. The static lateral stability characteristics of the various configurations at $\alpha = 0^{\circ}$ and $\alpha = 5.3^{\circ}$ are summarized in table II and are presented as functions of sweep angle and thickness ratio in figure 7. Both $C_{Y_{\psi}}$ and $C_{n_{\psi}}$ for most configurations tend to increase with lift coefficient. The effective dihedral $C_{l_{\psi}}$ is small and changes from negative to positive with increasing lift coefficient. The effect of nacelle installation is to increase the positive values of $C_{Y_{\psi}}$ and $C_{n_{\psi}}$ and the negative value of $C_{l_{\psi}}$. The effect of increasing the sweep angle or thickness ratio is to increase slightly the positive value of $C_{Y_{\psi}}$ and decrease the positive value of $C_{n_{\psi}}$. Table II shows that a change in Mach number from 1.60 to 2.01 had little effect on $C_{Y_{\psi}}$ but increased slightly the positive value of $C_{n_{\psi}}$.

Langley Aeronautical Laboratory
National Advisory Committee for Aeronautics
Langley Field, Va.

REFERENCES

1. Bielat, Ralph P., Harrison, Daniel E., and Coppolino, Domenic A.: An Investigation at Transonic Speeds of the Effects of Thickness Ratio and of Thickened Root Sections on the Aerodynamic Characteristics of Wings With 47° Sweepback, Aspect Ratio 3.5, and Taper Ratio 0.2 in the Slotted Test Section of the Langley 8-Foot High-Speed Tunnel. NACA RM L51I04a, 1951.

2. Bielat, Ralph P.: Transonic Wind-Tunnel Investigation of the Aerodynamic Characteristics of Three 4-Percent-Thick Wings of Sweepback Angles 10.8°, 35°, and 47°, Aspect Ratio 3.5, and Taper Ratio 0.2 in Combination With a Body. NACA RM L52B08, 1952.

3. Robinson, Ross B., and Driver, Cornelius: Aerodynamic Characteristics at Supersonic Speeds of a Series of Wing-Body Combinations Having Cambered Wings With an Aspect Ratio of 3.5 and a Taper Ratio of 0.2. Effects of Sweep Angle and Thickness Ratio on the Aerodynamic Characteristics in Pitch at $M = 1.60$. NACA RM L51K16a, 1952.

4. Robinson, Ross B.: Aerodynamic Characteristics at Supersonic Speeds of a Series of Wing-Body Combinations Having Cambered Wings With an Aspect Ratio of 3.5 and a Taper Ratio of 0.2. Effects of Sweep Angle and Thickness Ratio on the Aerodynamic Characteristics in Pitch at $M = 2.01$. NACA RM L52E09, 1952.

5. Hasel, Lowell E., and Sevier, John R., Jr.: Aerodynamic Characteristics at Supersonic Speeds of a Series of Wing-Body Combinations Having Cambered Wings With an Aspect Ratio of 3.5 and a Taper Ratio of 0.2. Effect at $M = 1.60$ of Nacelle Shape and Position on the Aerodynamic Characteristics in Pitch of Two Wing-Body Combinations With 47° Sweptback Wings. NACA RM L51K14a, 1952.

6. Driver, Cornelius: Aerodynamic Characteristics at Supersonic Speeds of a Series of Wing-Body Combinations Having Cambered Wings With an Aspect Ratio of 3.5 and a Taper Ratio of 0.2. Effect at $M = 2.01$ of Nacelle Shape and Position on the Aerodynamic Characteristics in Pitch of Two Wing-Body Combinations With 47° Sweptback Wings. NACA RM L52F03, 1952.

7. Spearman, M. Leroy, and Hilton, John H., Jr.: Aerodynamic Characteristics at Supersonic Speeds of a Series of Wing-Body Combinations Having Cambered Wings With an Aspect Ratio of 3.5 and a Taper Ratio of 0.2. Effects of Sweep Angle and Thickness Ratio on the Static Lateral Stability Characteristics at $M = 1.60$. NACA RM L51K15a, 1952.

[redacted]

TABLE I.- AIRFOIL COORDINATES FOR THE VARIOUS WINGS

$\frac{t}{c} = 0.04$

x/c	y/c upper surface	y/c lower surface
0	0	0
.5	.411	.245
.75	.499	.271
1.25	.665	.289
2.5	.962	.324
5.0	1.435	.367
7.5	1.776	.429
10	2.039	.472
15	2.423	.577
20	2.642	.682
25	2.800	.787
30	2.887	.892
35	2.983	.997
40	2.992	1.006
45	2.940	1.041
50	2.852	1.006
55	2.712	.945
60	2.511	.857
65	2.265	.761
70	1.986	.674
75	1.680	.577
80	1.356	.481
85	1.041	.385
90	.726	.289
95	.402	.201
100	.105	.105
Tangent Point	80.00	60.00
L.E. radius = 0.0016c		

$\frac{t}{c} = 0.06$

x/c	y/c upper surface	y/c lower surface
0	0.061	0
.5	.577	.376
.75	.717	.446
1.25	.919	.534
2.5	1.304	.621
5.0	1.872	.761
7.5	2.318	.857
10	2.668	.980
15	3.150	1.269
20	3.482	1.496
25	3.701	1.697
30	3.858	1.846
35	3.946	1.960
40	3.981	2.021
45	3.937	2.030
50	3.823	1.977
55	3.613	1.872
60	3.342	1.697
65	3.018	1.487
70	2.651	1.277
75	2.231	1.059
80	1.785	.849
85	1.339	.639
90	.892	.420
95	.446	.210
100	0	0
L.E. radius = 0.0024c		

$\frac{t}{c} = 0.09$

x/c	y/c upper surface	y/c lower surface
0	0.156	0
.5	.846	.574
.75	1.021	.680
1.25	1.283	.846
2.5	1.789	1.069
5.0	2.537	1.400
7.5	3.111	1.662
10	3.577	1.896
15	4.244	2.352
20	4.705	2.751
25	5.045	3.052
30	5.288	3.276
35	5.415	3.441
40	5.473	3.529
45	5.424	3.519
50	5.249	3.422
55	4.967	3.208
60	4.579	2.916
65	4.102	2.566
70	3.568	2.197
75	2.975	1.837
80	2.382	1.468
85	1.789	1.098
90	1.186	.739
95	.593	.369
100	0	0
L.E. radius = 0.0056c		

Thickened root

x/c	Root station	
	y/c upper surface	y/c lower surface
0	0.301	0
.5	1.120	.754
.75	1.335	.904
1.25	1.658	1.141
2.5	2.261	1.507
5.0	3.208	2.024
7.5	3.919	2.433
10	4.500	2.799
15	5.362	3.445
20	5.965	3.984
25	6.395	4.414
30	6.718	4.716
35	6.912	4.910
40	6.977	5.017
45	6.912	4.996
50	6.675	4.823
55	6.288	4.522
60	5.771	4.113
65	5.168	3.618
70	4.457	3.101
75	3.725	2.584
80	2.929	2.067
85	2.239	1.550
90	1.486	1.034
95	.732	.517
100	0	0
L.E. radius = 0.0099c		

NACA

[redacted]

TABLE II.- SUMMARY OF STATIC-LATERAL-STABILITY DERIVATIVES ($\psi = 0^{\circ}$)

Λ, deg	t/c	Nacelles	α, deg	M = 1.60			M = 2.01		
				C_{Y_ψ}	C_{n_ψ}	C_{l_ψ}	C_{Y_ψ}	C_{n_ψ}	C_{l_ψ}
10.8	0.04	Off	0	-------	-------	--------	0.0018	0.00059	-0.00008
35	.04	Off	0	-------	-------	--------	.0018	.00048	-.00016
47	.04	Off	0	-------	-------	--------	.0020	.00043	-.00025
47	.06	Off	0	-------	-------	--------	.0021	.00038	-.00025
47	.09	Off	0	-------	-------	--------	.0023	.00025	-.00023
47	0.12 to 0.06	Off	0	-------	-------	--------	.0025	.00030	-.00025
47	.06	On	0	-------	-------	--------	.0058	.00095	-.00040
10.8	.04	Off	5.3	0.0012	0.00057	-0.00010	.0013	.00058	.00008
35	.04	Off	5.3	.0018	.00046	0	.0018	.00055	-.00005
47	.04	Off	5.3	.0020	.00040	.00003	.0020	.00053	-.00006
47	.06	Off	5.3	.0022	.00030	-.00003	.0021	.00035	0
47	.09	Off	5.3	.0026	.00017	-.00011	.0023	.00025	.00002
47	0.12 to 0.06	Off	5.3	-------	-------	--------	.0025	.00030	0
47	.06	On	5.3	.0076	.00122	-.00020	.0058	.00106	-.00050
Body alone			5.3	.0015	.00055	.00004	.0013	.00003	.00005

NACA

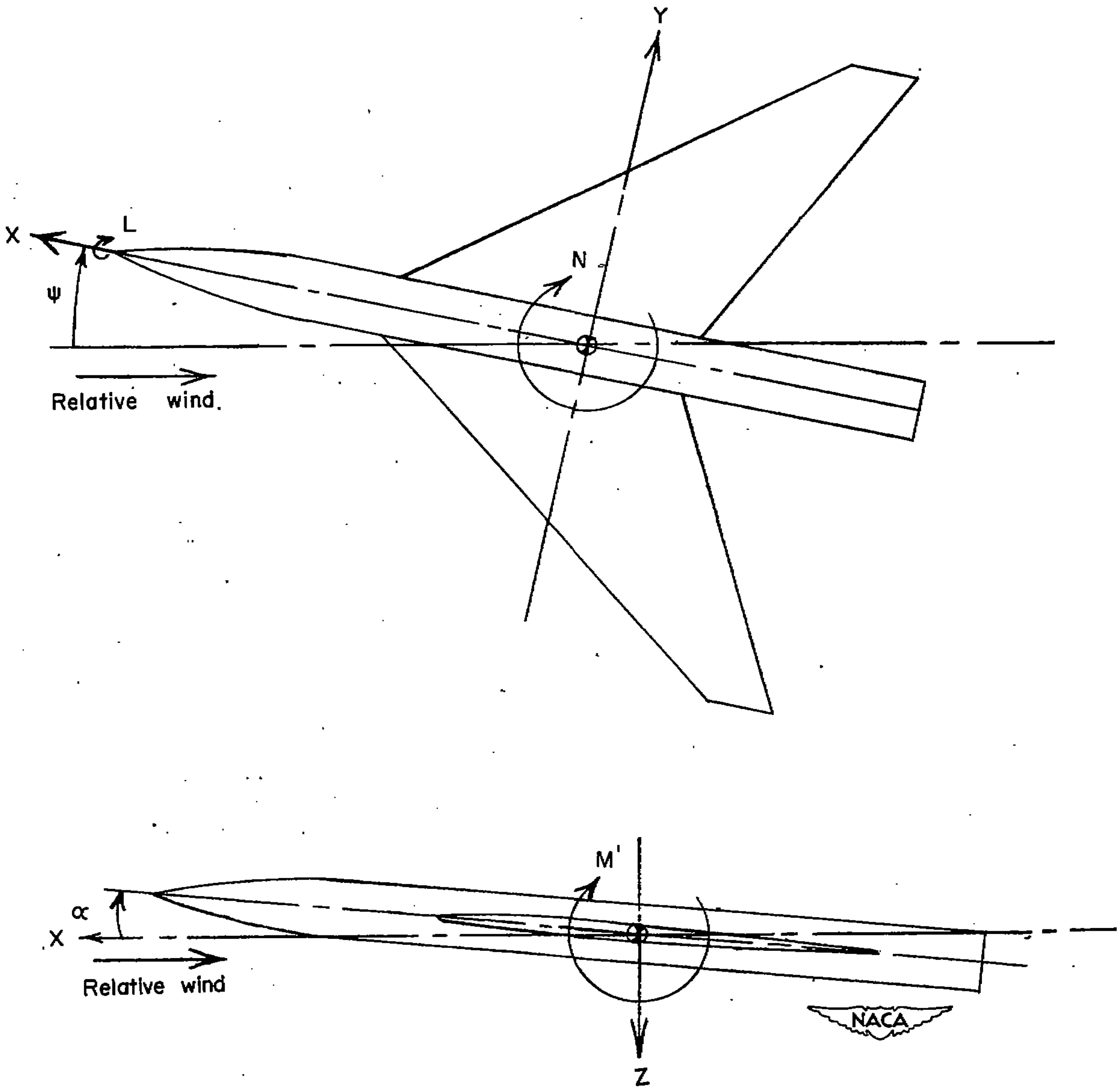

Figure 1.- System of stability axes. Arrows indicate positive values.

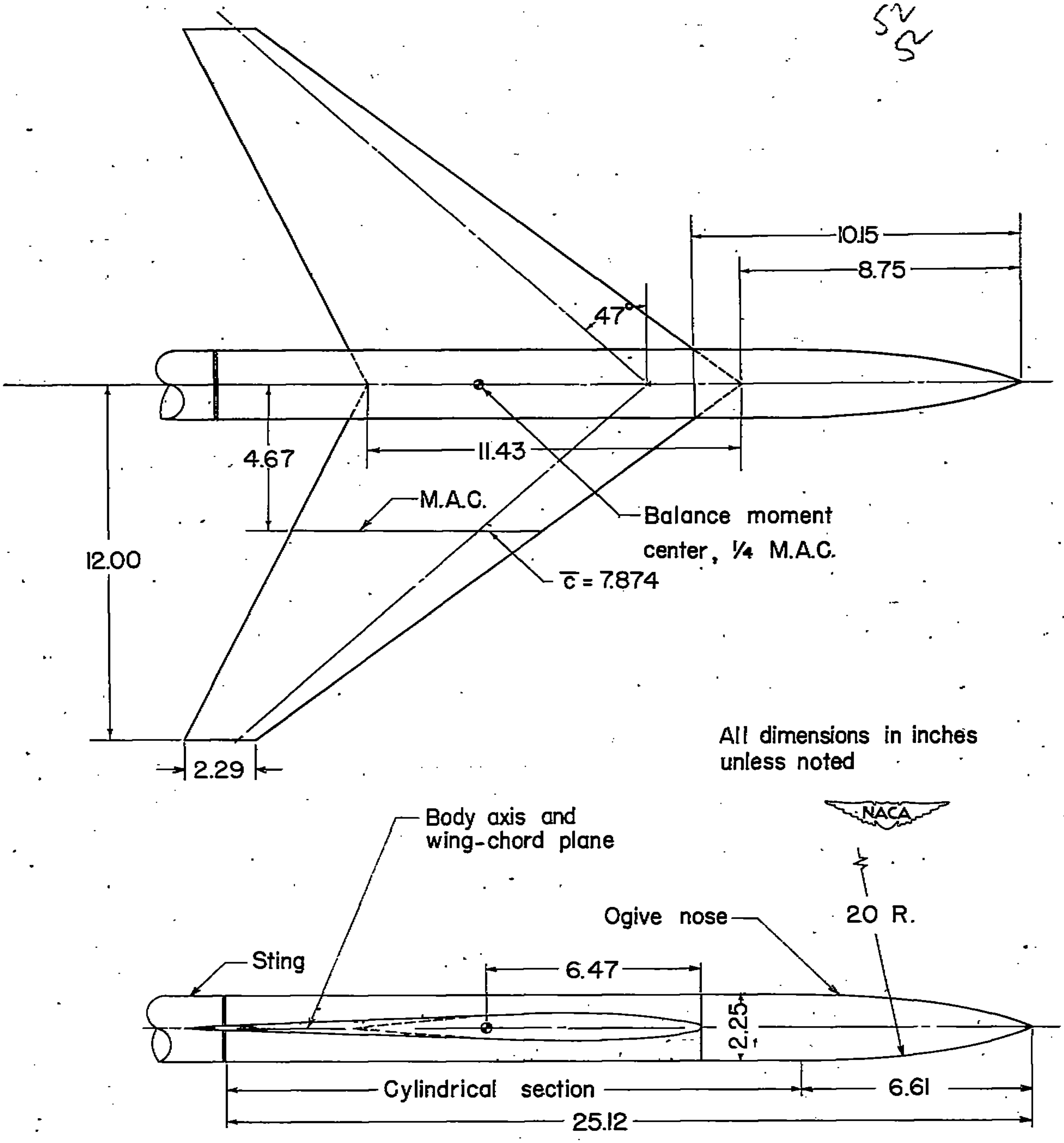

(a) Wing-body arrangement.

Figure 2.- Details of model configurations.

[redacted]

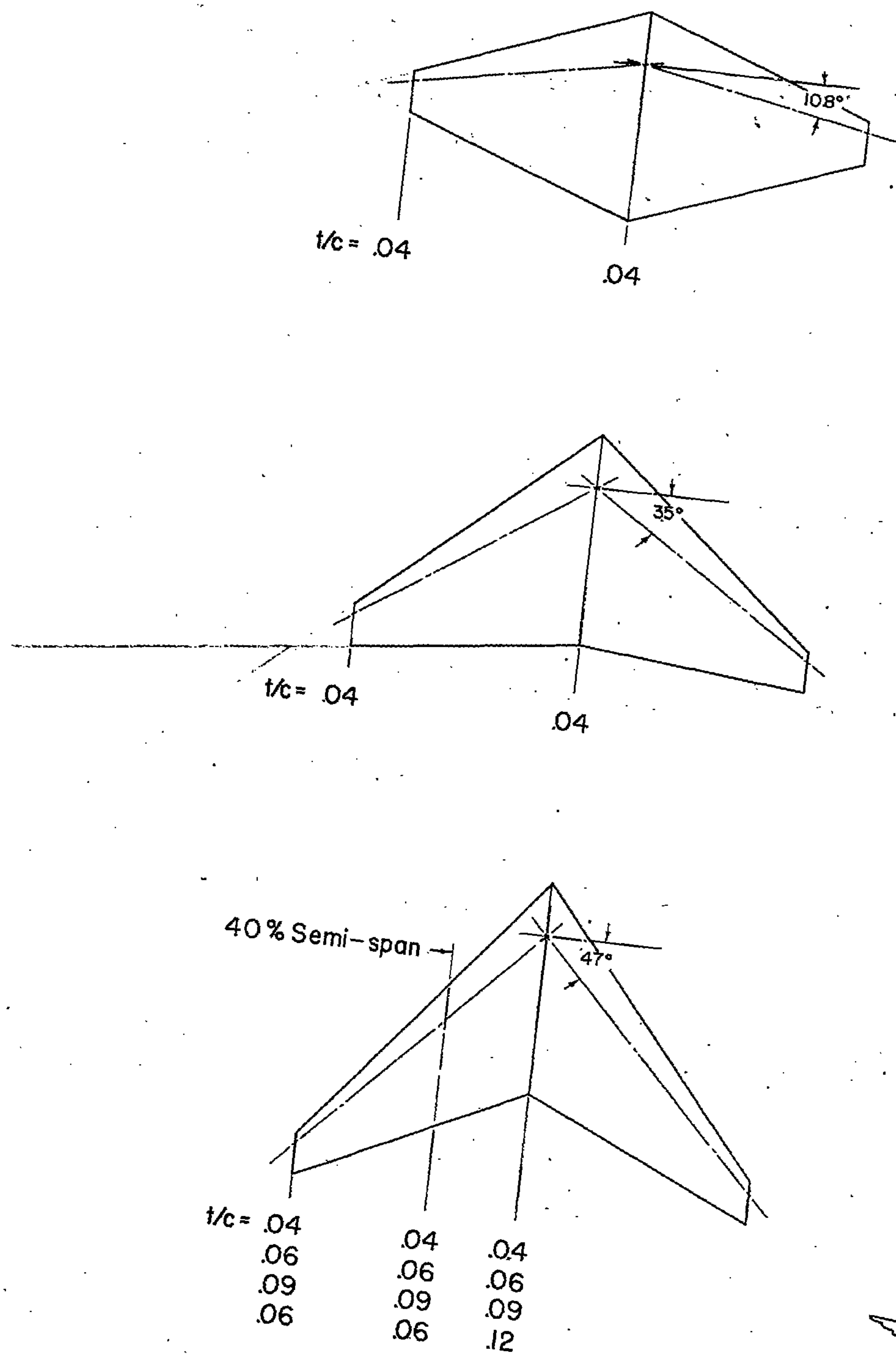

Aspect Ratio	3.5
Taper Ratio	0.2
Span, inches	24
Area, sq. feet	1.143

(b) Details of wings.

Figure 2.- Continued.

[redacted]

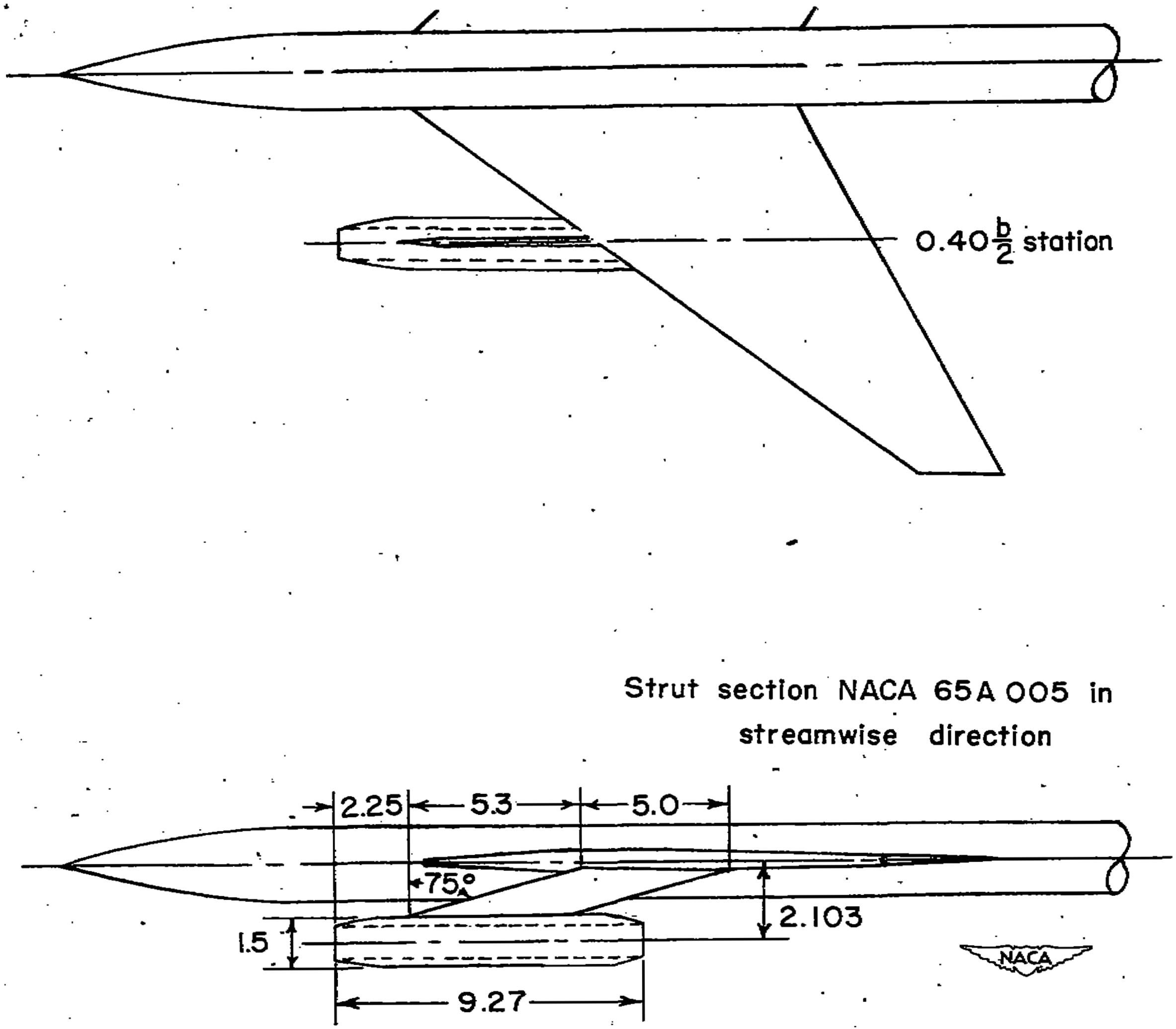

(c) Details of nacelle installation on $\Lambda = 47^{\circ}$, $\frac{t}{c} = 0.06$ wing.

Figure 2.- Concluded.

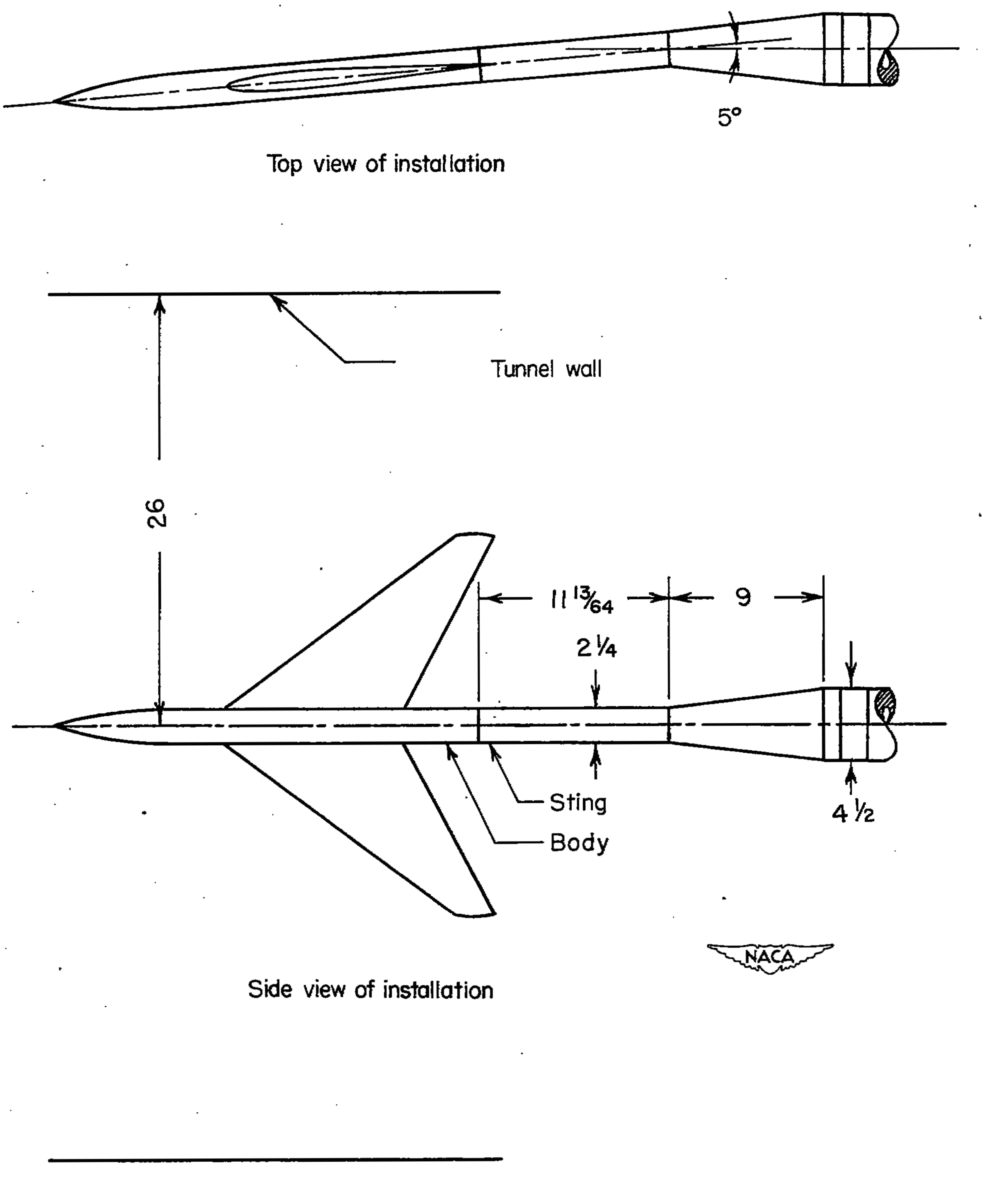

Figure 3.- Details of model sting support. All dimensions in inches unless noted.

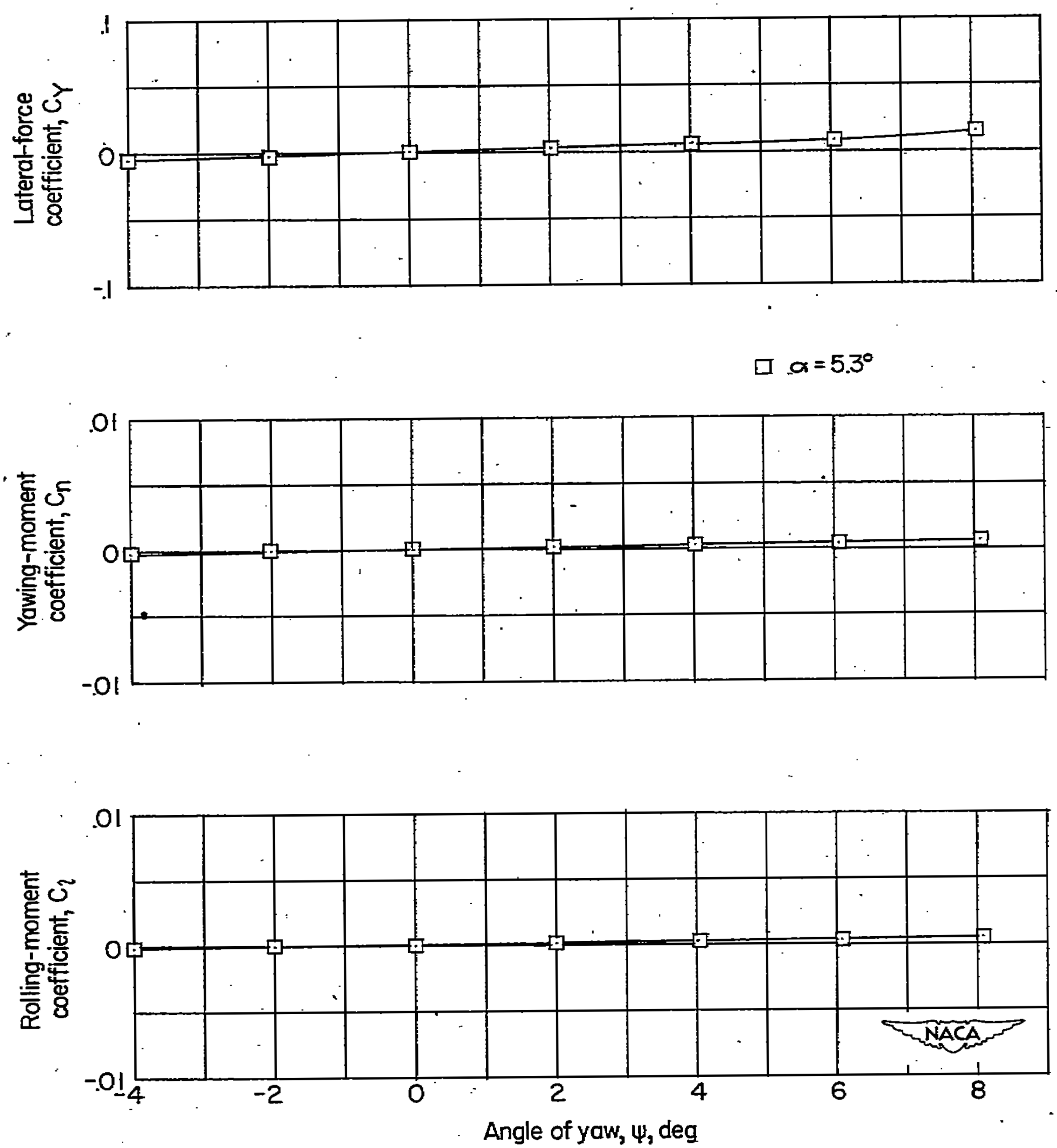

(a) Body alone.

Figure 4.- Aerodynamic characteristics in yaw for various configurations at $M = 2.01$.

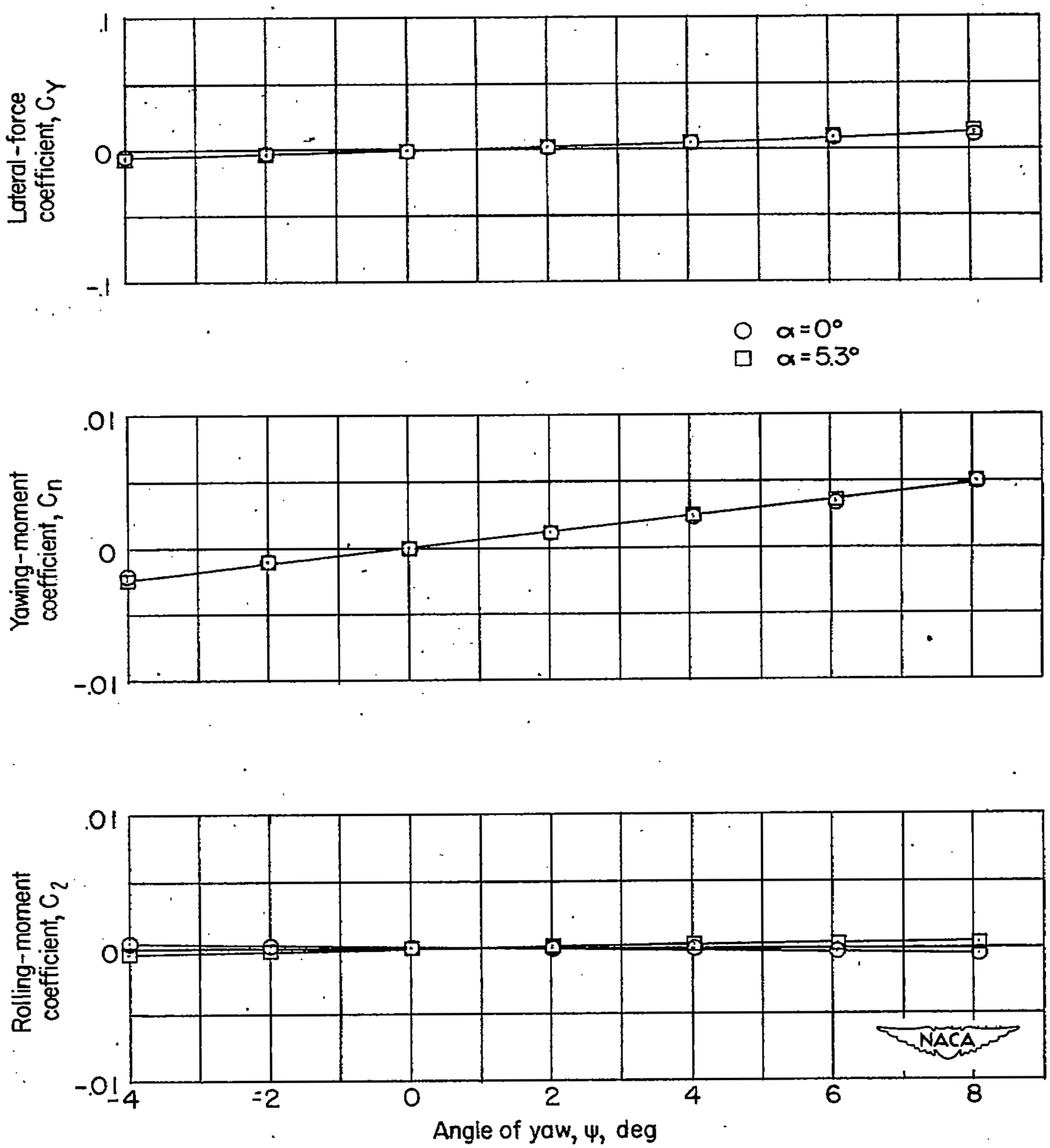

(b) $\Lambda = 10.8$; $\frac{t}{c} = 0.04$.

Figure 4.- Continued.

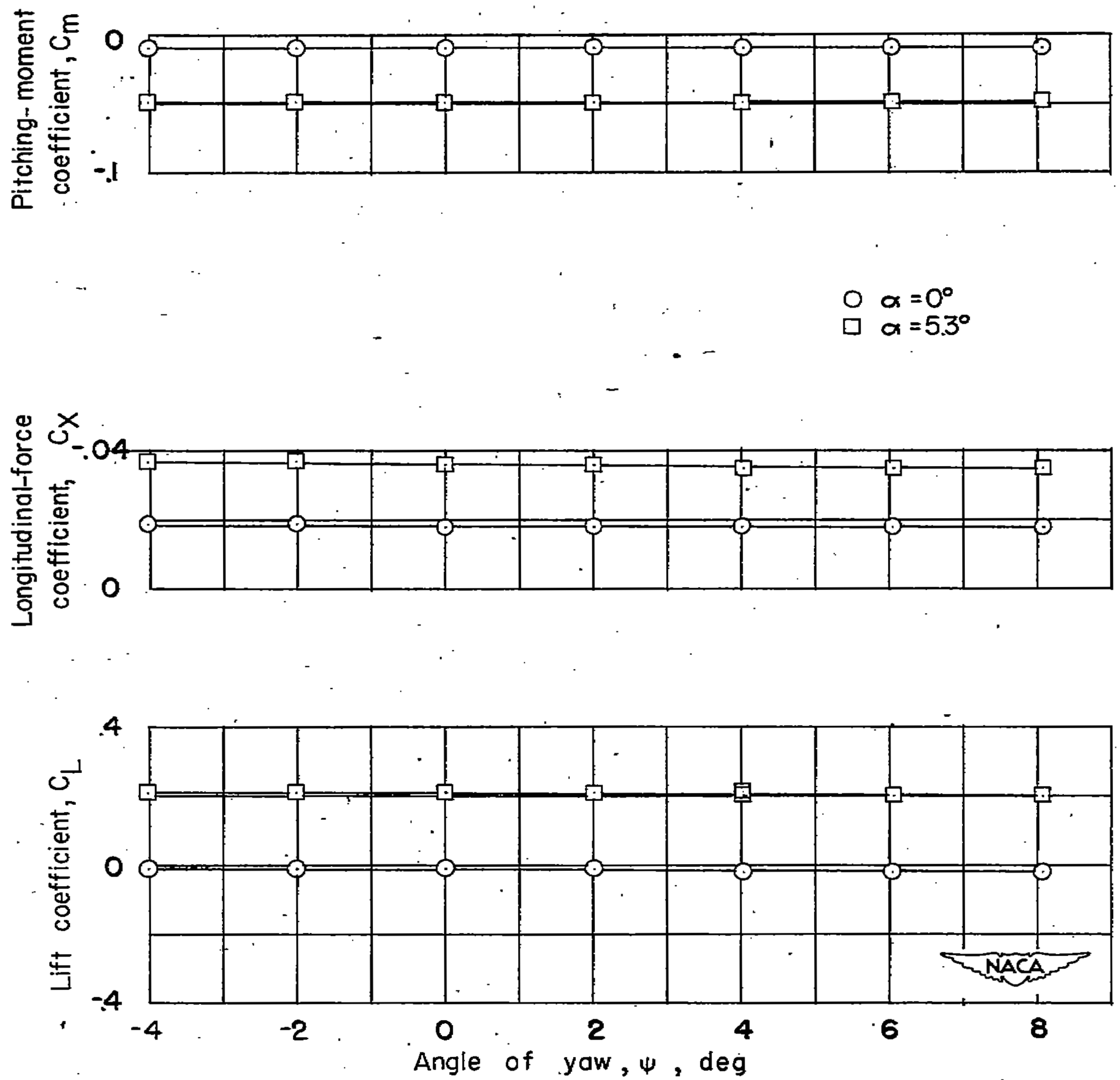

(b) Concluded.

Figure 4.- Continued.

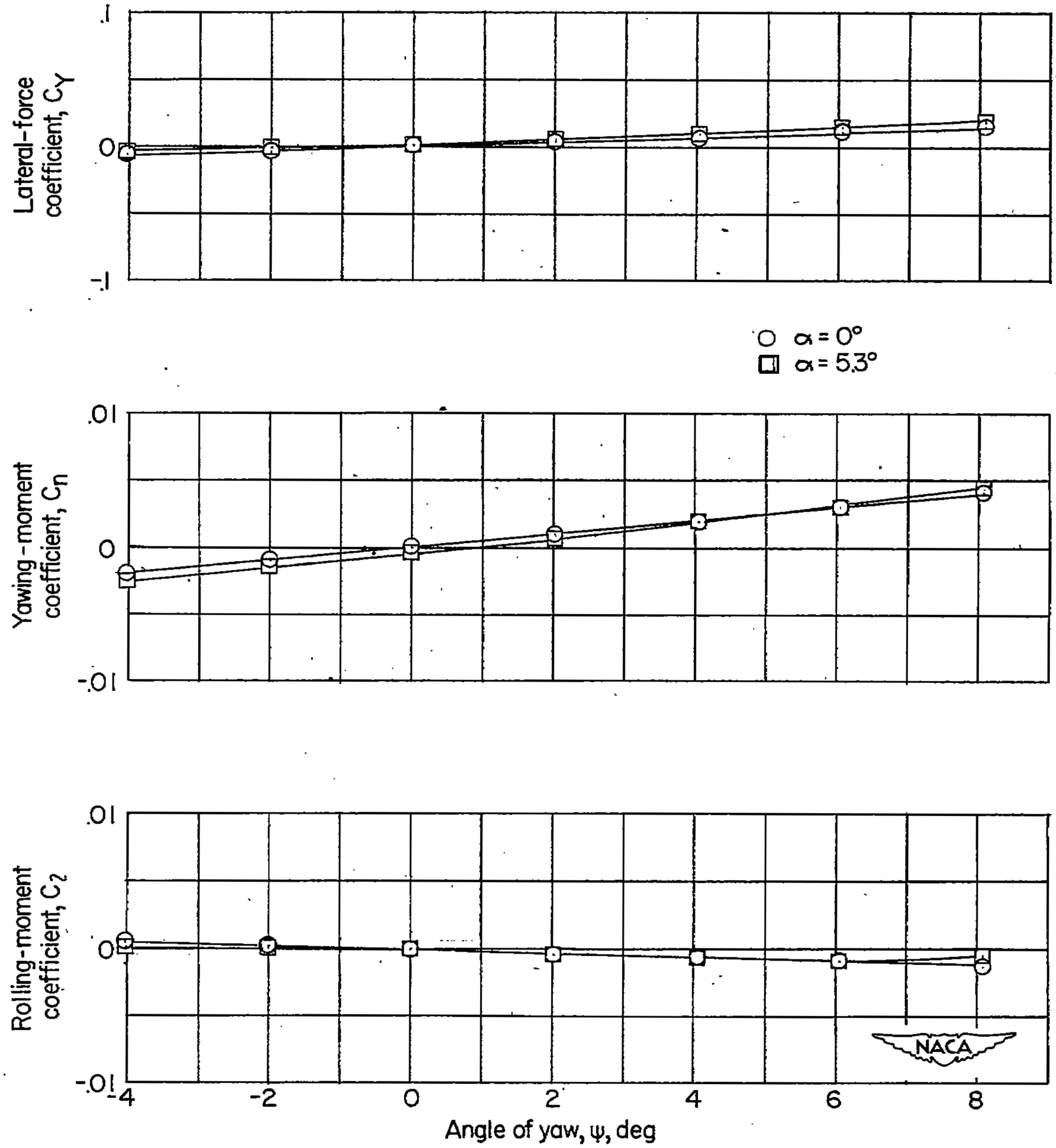

(c) $\Lambda = 35^{\circ}$; $\frac{t}{c} = 0.04$.

Figure 4.- Continued.

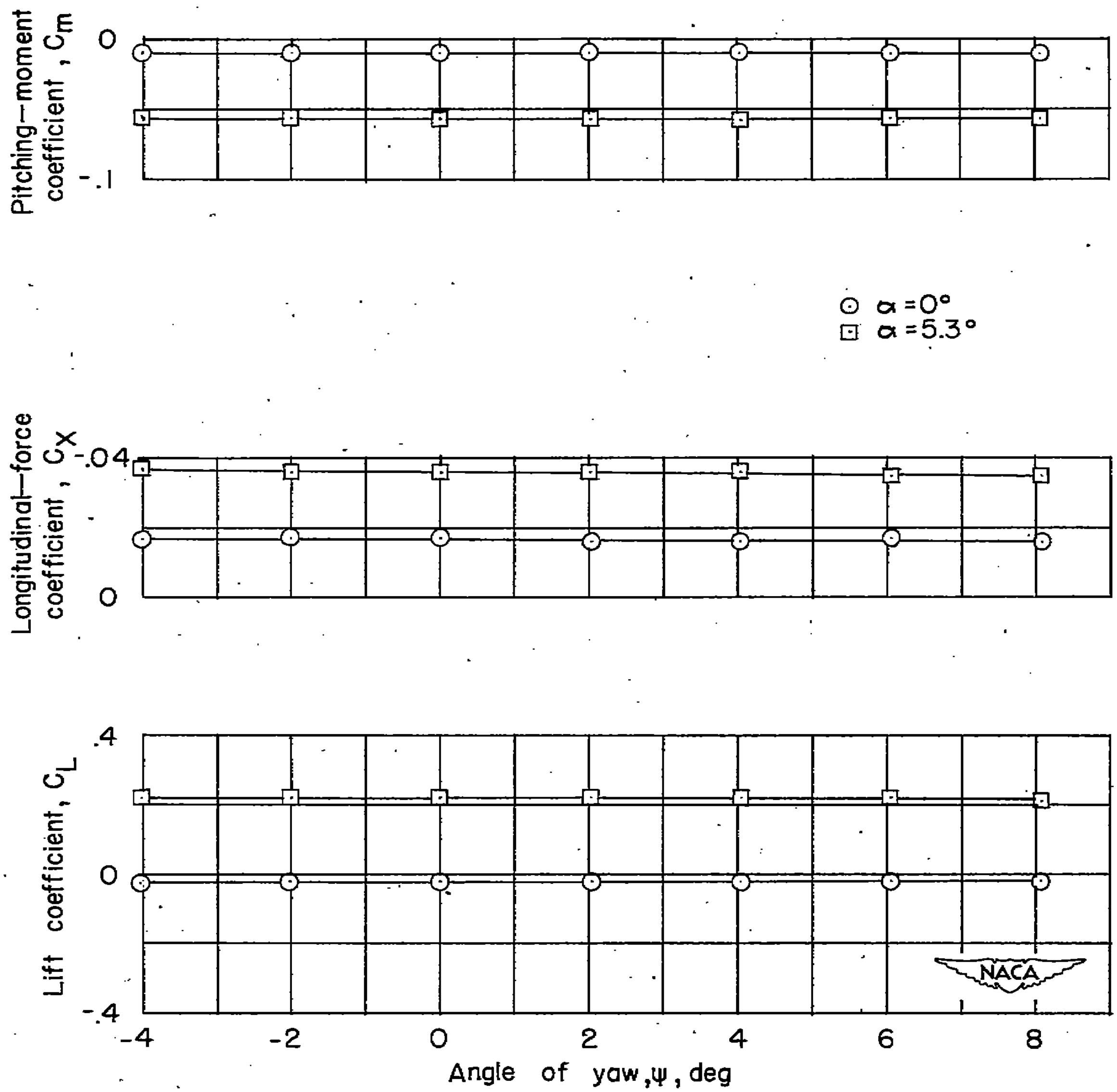

(c) Concluded.

Figure 4.- Continued.

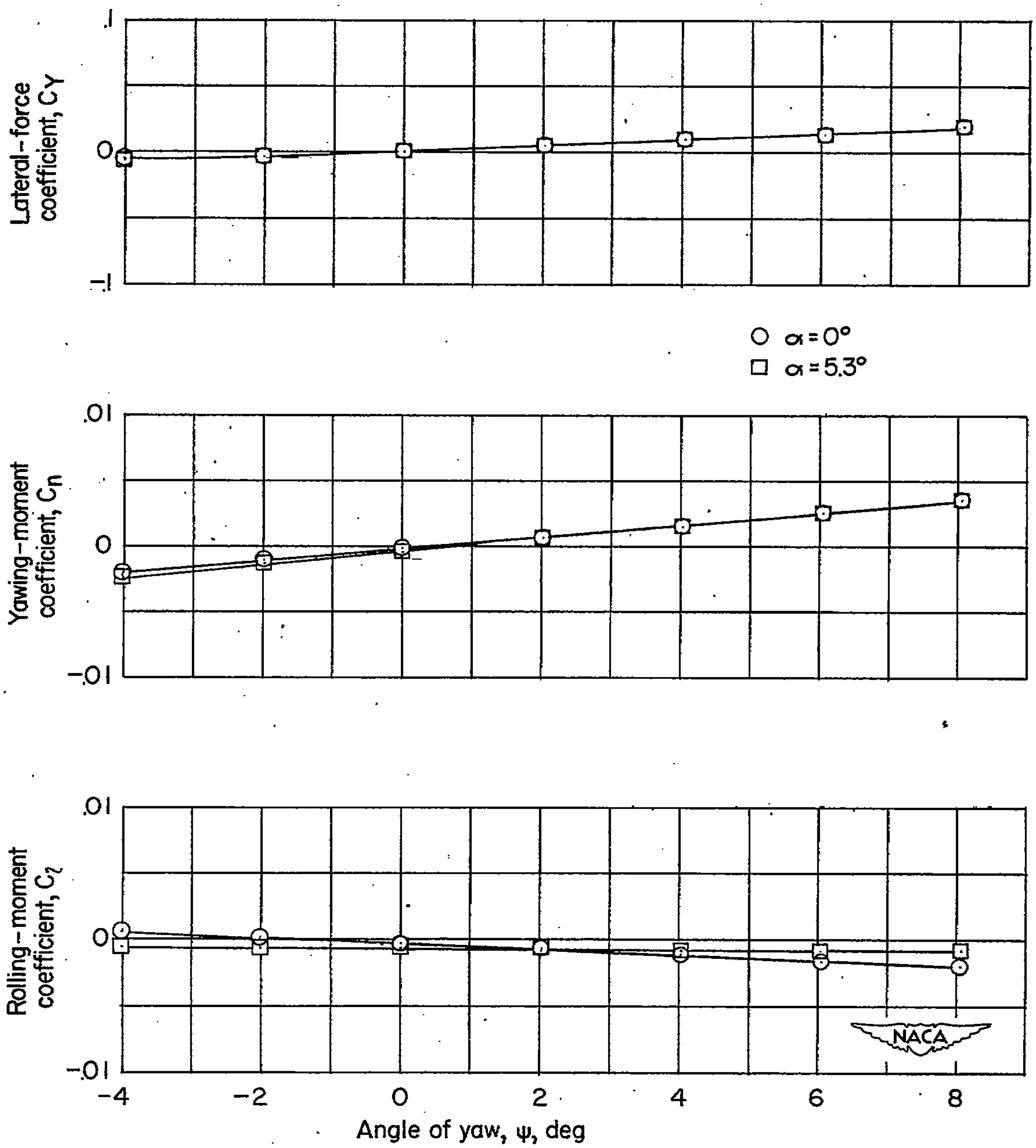

(d) $\Lambda = 47^{\circ}$; $\frac{t}{c} = 0.04$.

Figure 4.- Continued.

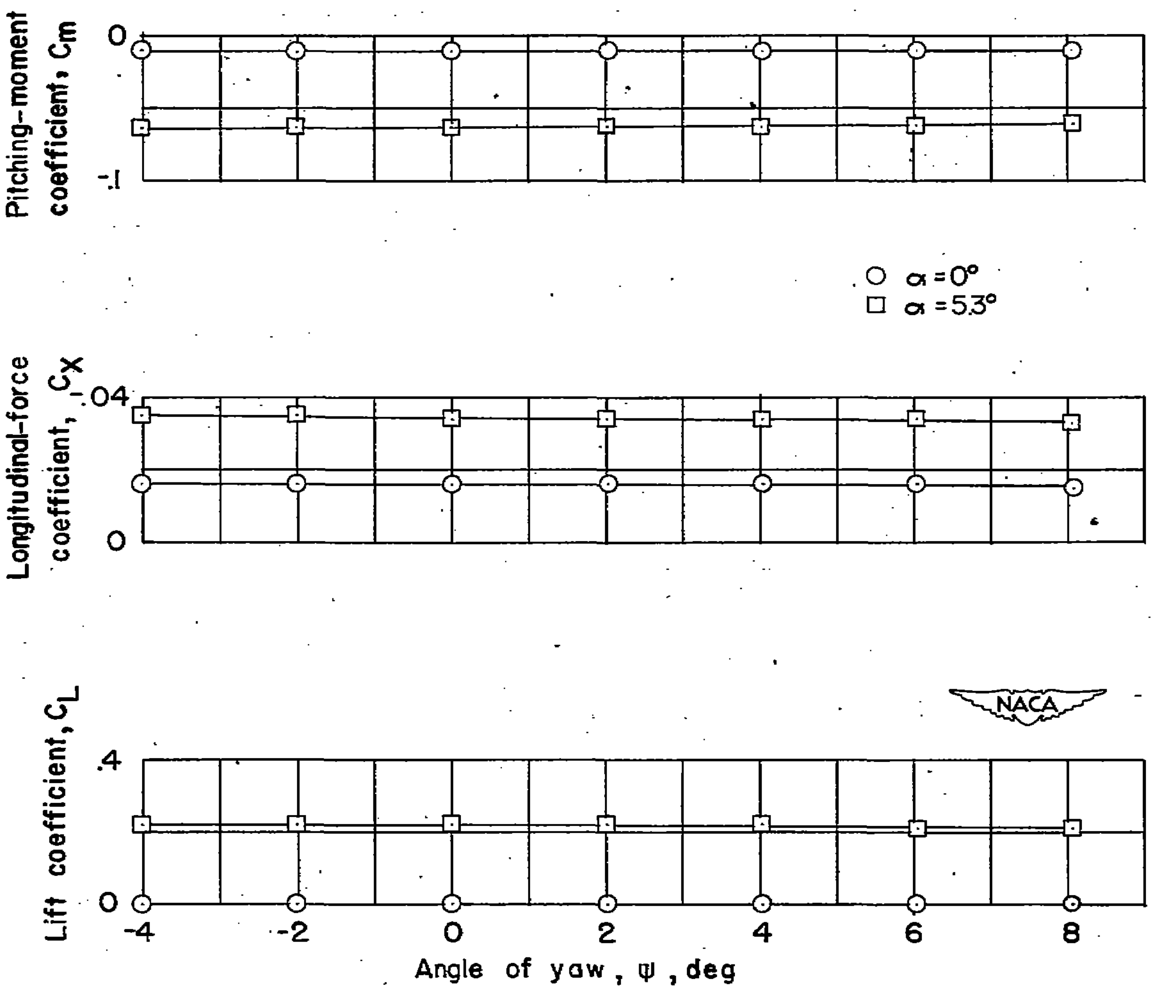

(d) Concluded.

Figure 4.- Continued.

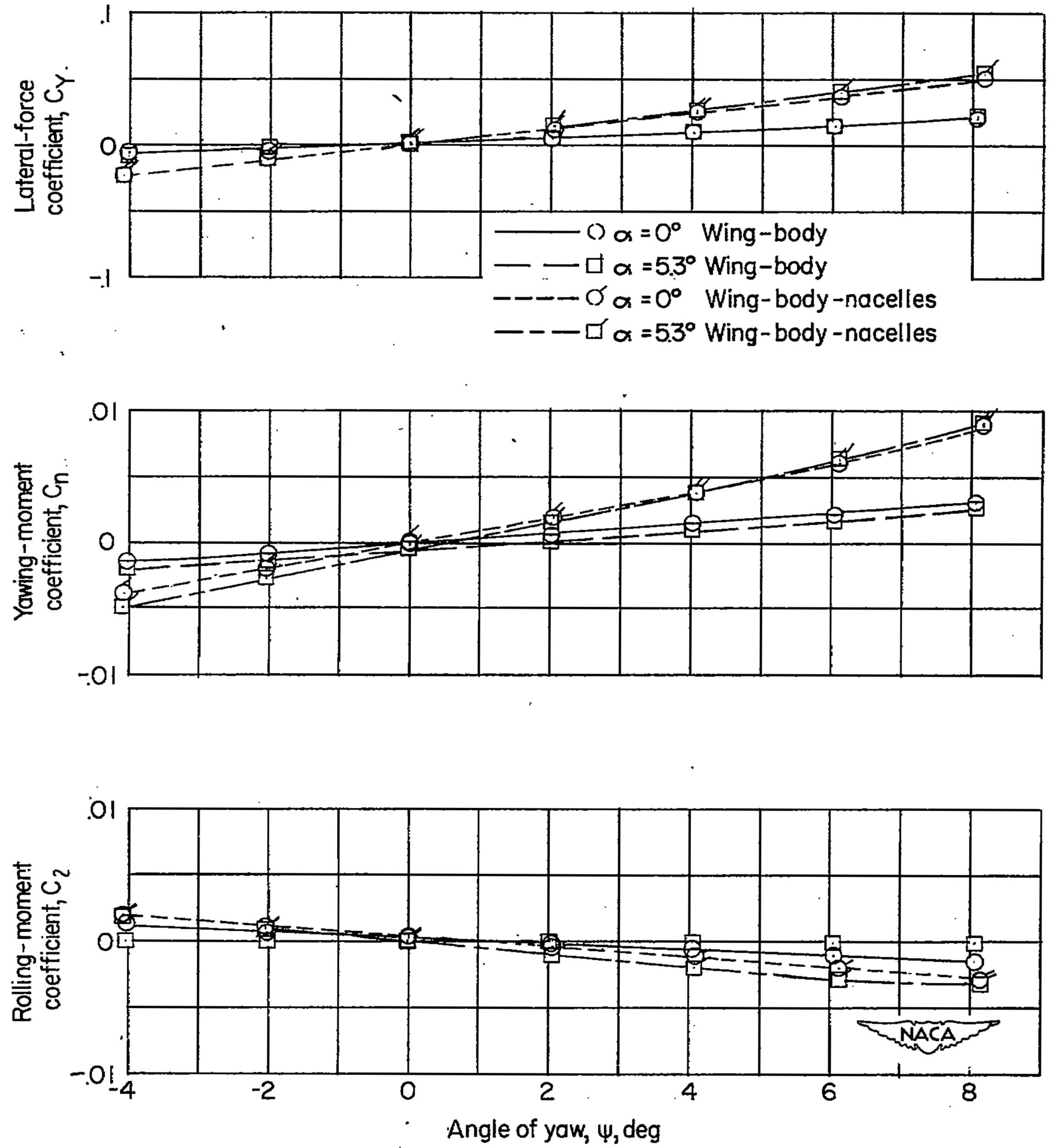

(e) $\Lambda = 47^{\circ}$; $\frac{t}{c} = 0.06$.

Figure 4.- Continued.

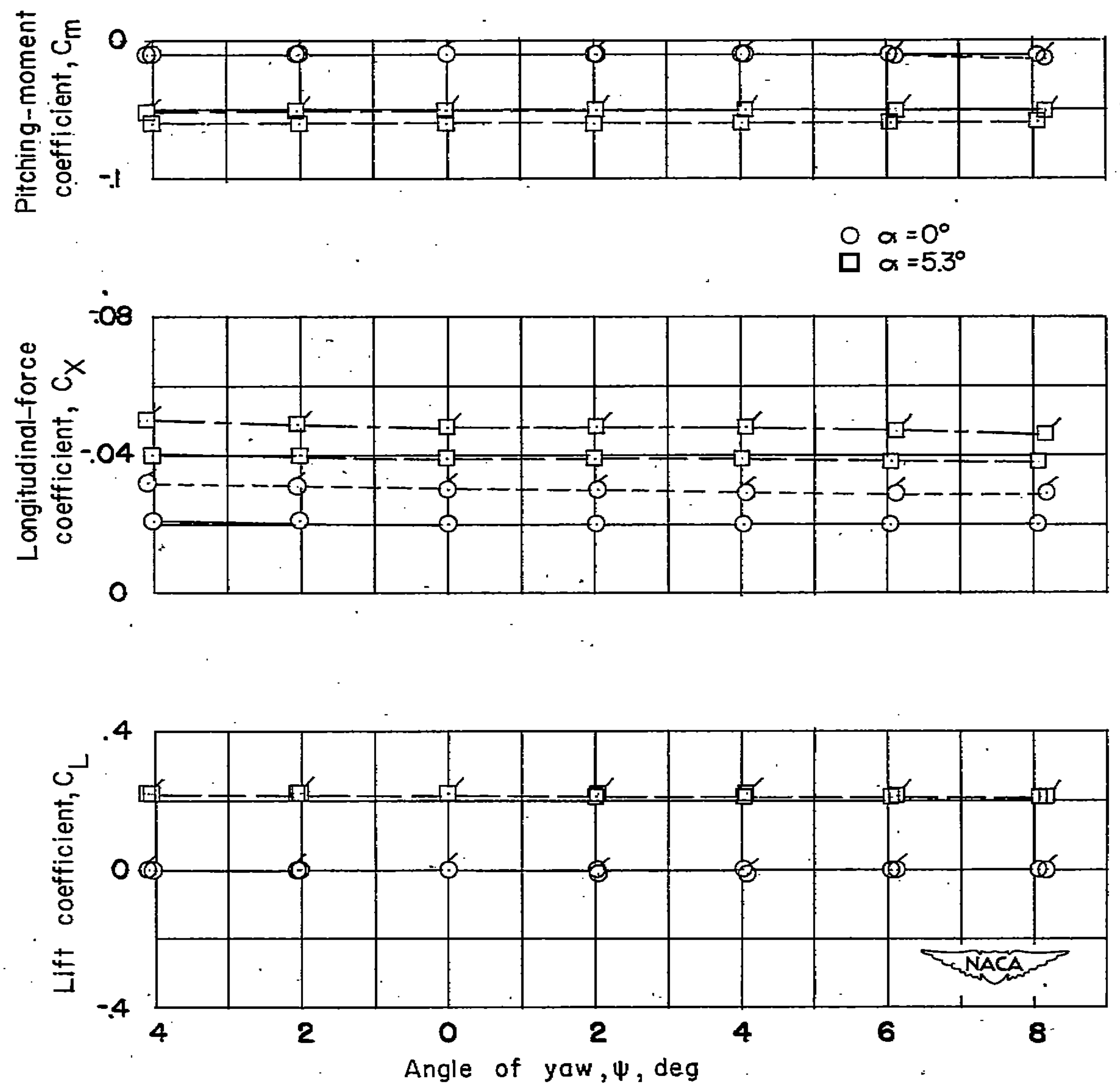

(e) Concluded.

Figure 4.- Continued.

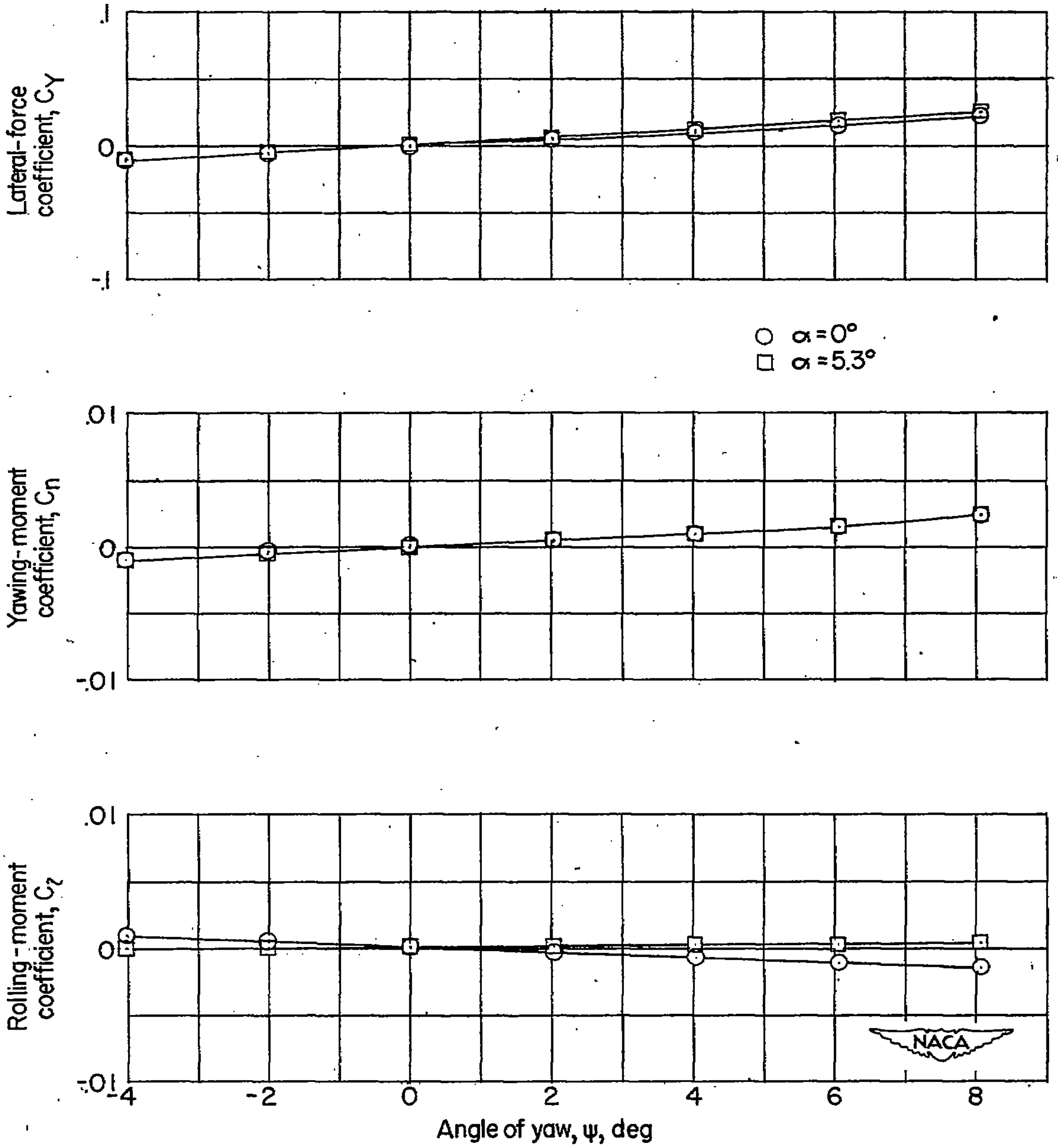

(f) $\Lambda = 47^{\circ}$; $\frac{t}{c} = 0.09$.

Figure 4.- Continued.

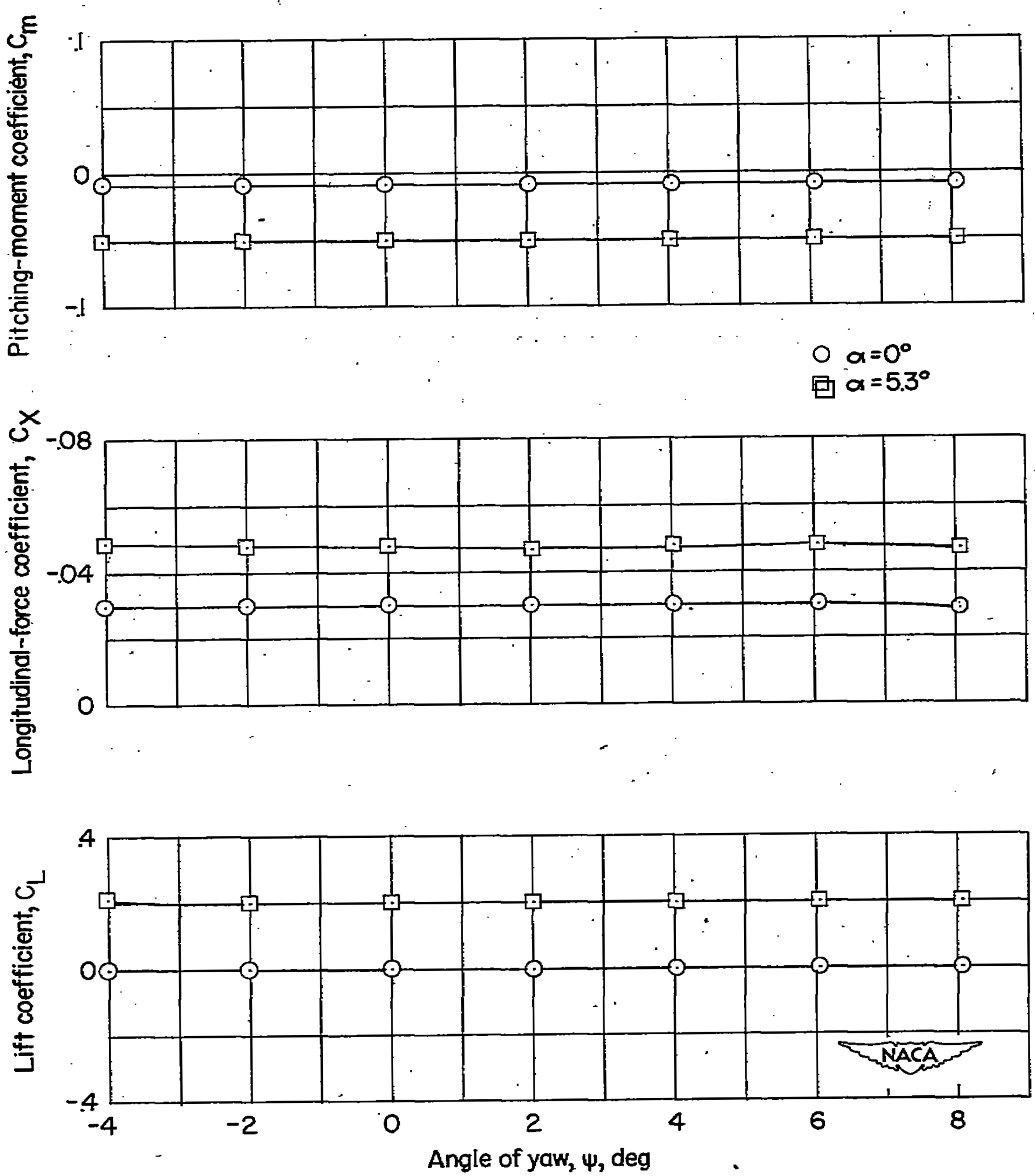

(f) Concluded.

Figure 4.- Continued.

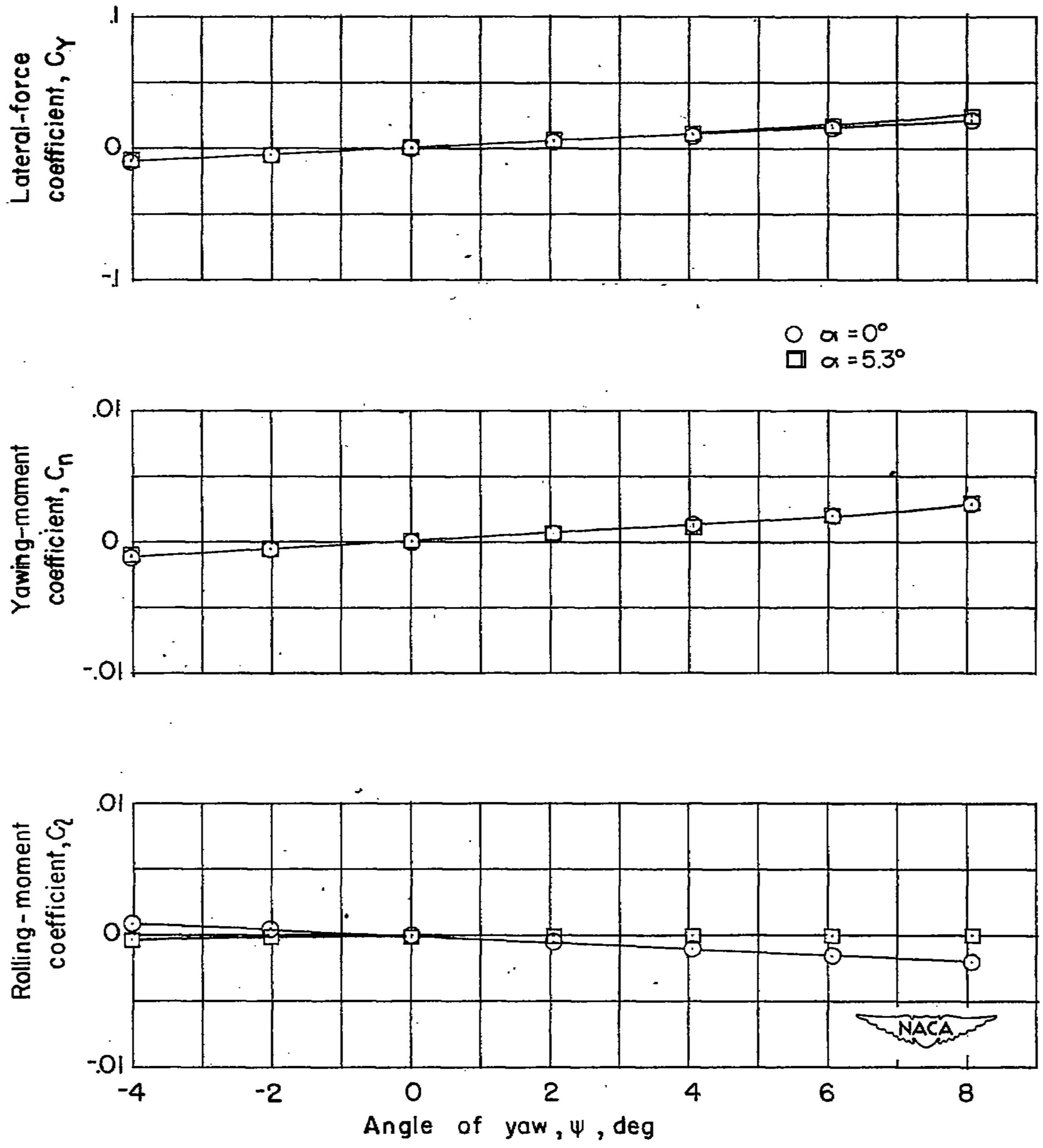

(g) $\Lambda = 47^{\circ}$; $\frac{t}{c} = 0.12$ to 0.06.

Figure 4.- Continued.

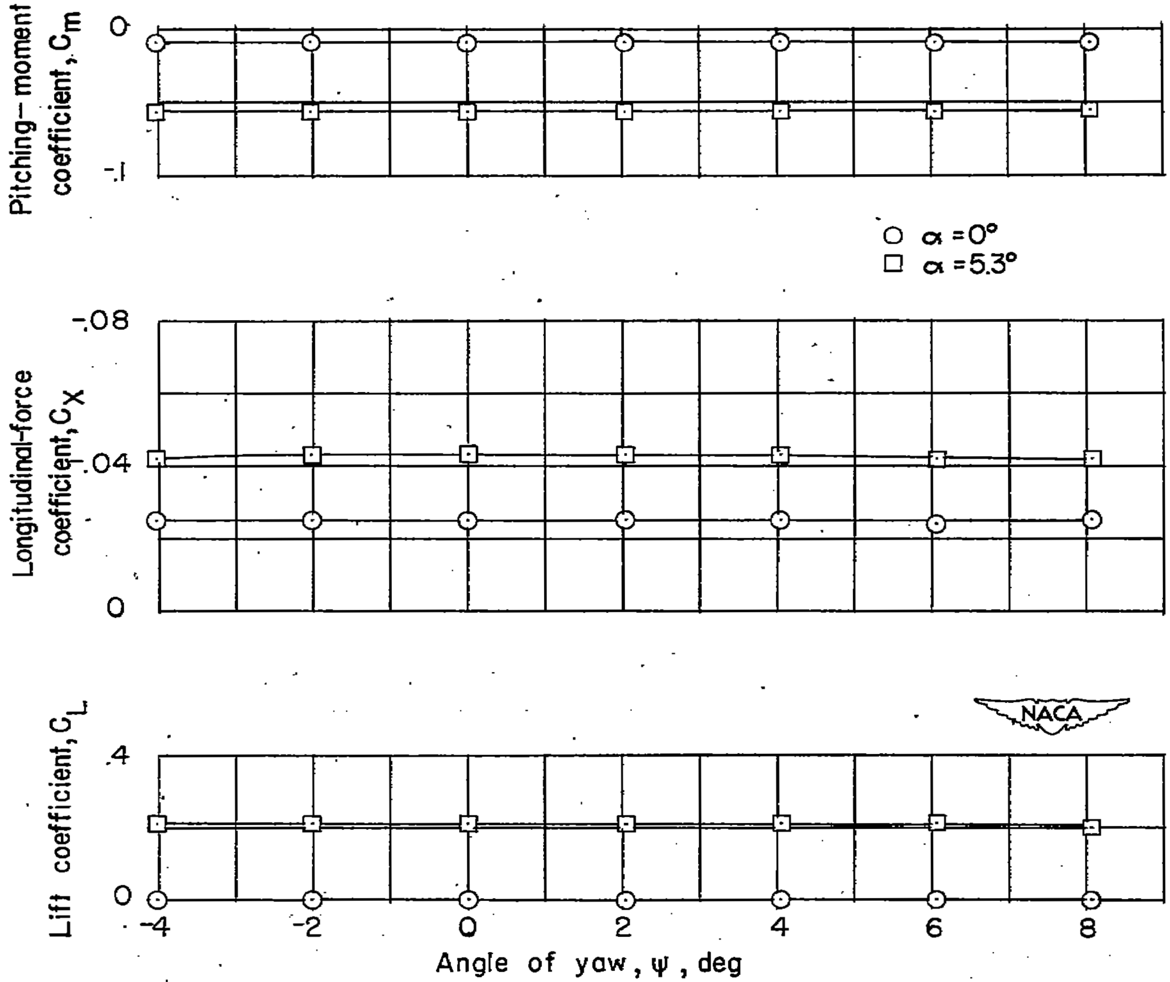

(g) Concluded.

Figure 4.- Concluded.

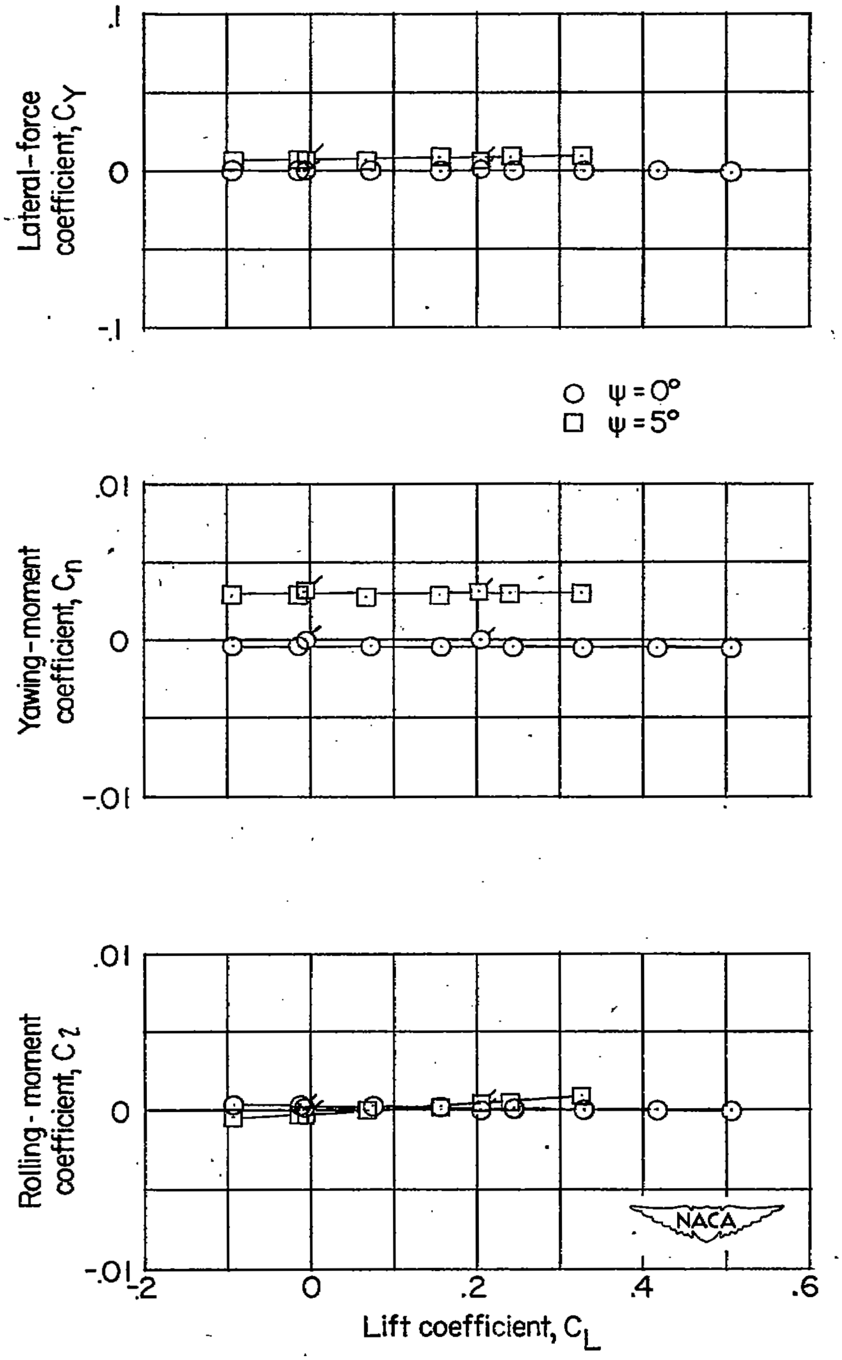

(a) $\Lambda = 10.8^{\circ}$; $\frac{t}{c} = 0.04$.

Figure 5.- Effect of yaw on the lateral characteristics in pitch for various configurations. Flagged symbols are values from yaw tests.

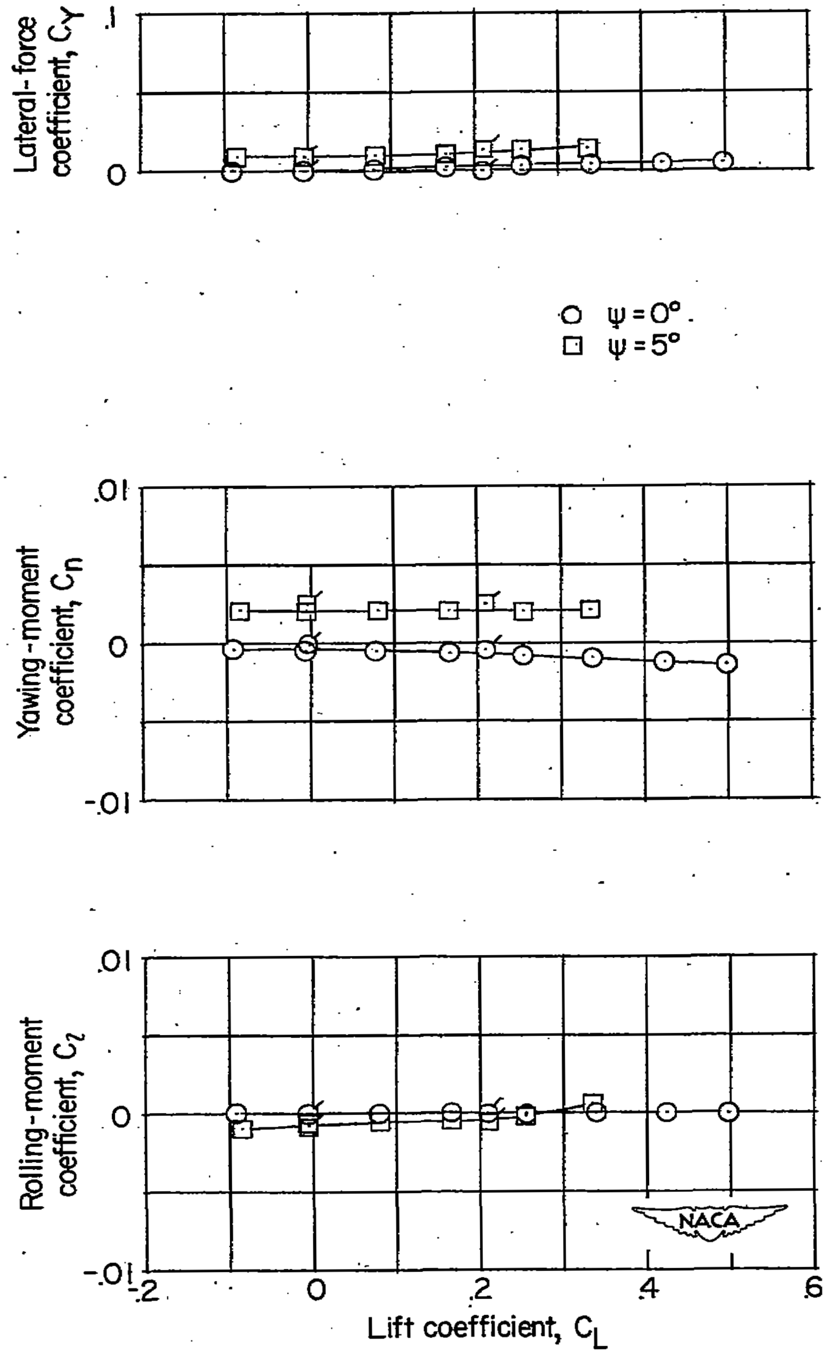

(b) $\Lambda = 35^{\circ}$; $\frac{t}{c} = 0.04$.

Figure 5.- Continued.

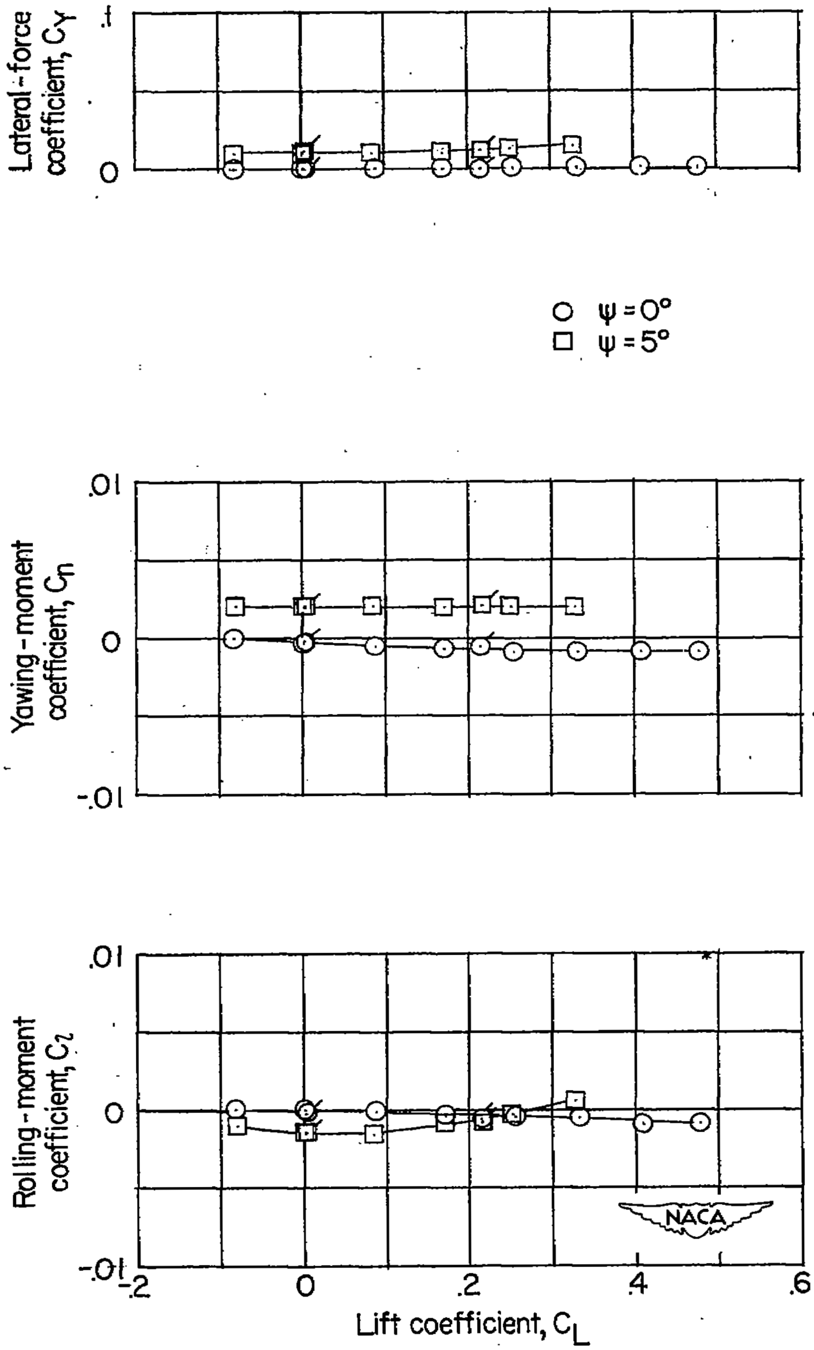

(c) $\Lambda = 47^{\circ}$; $\frac{t}{c} = 0.04$.

Figure 5.- Continued.

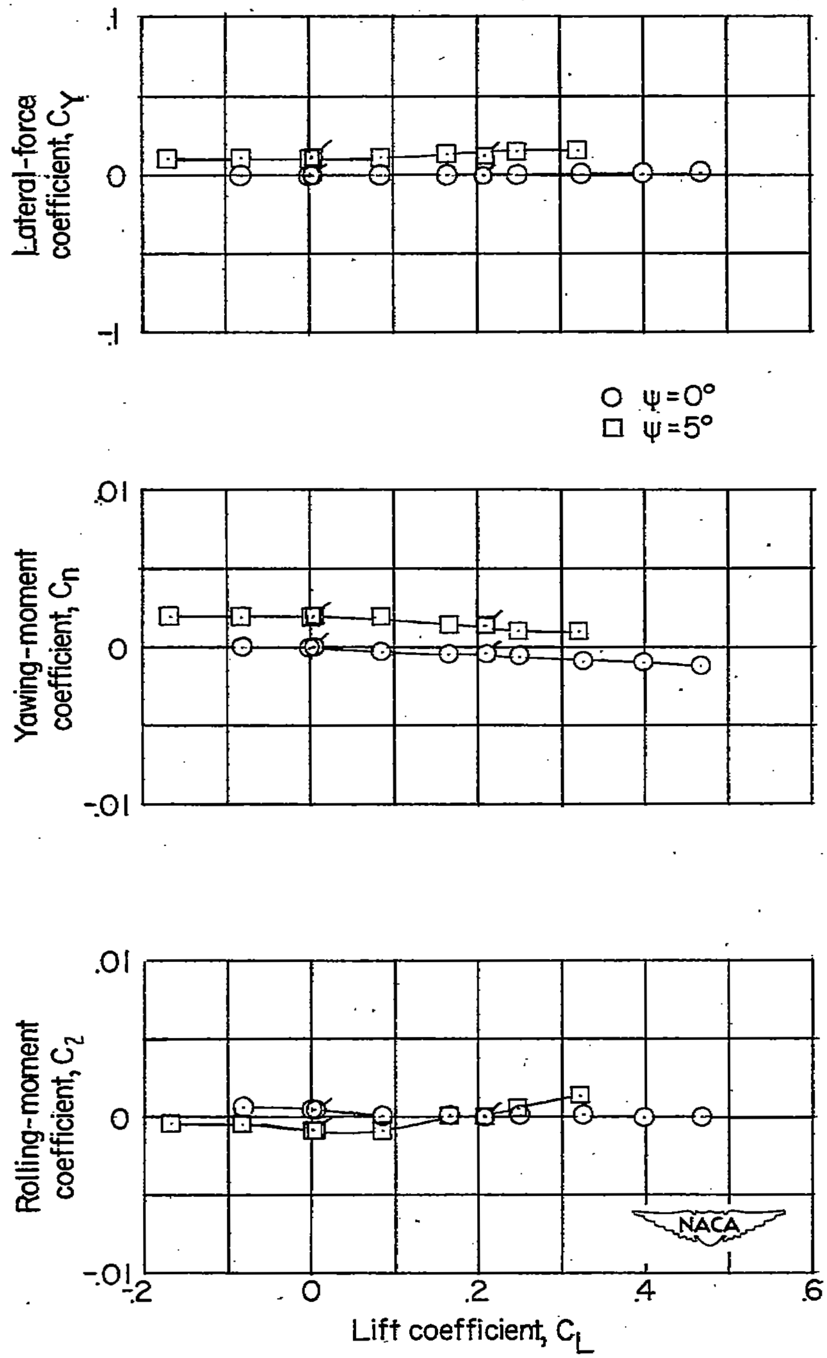

(d) $\Lambda = 47^{\circ}$; $\frac{t}{c} = 0.06$.

Figure 5.- Continued.

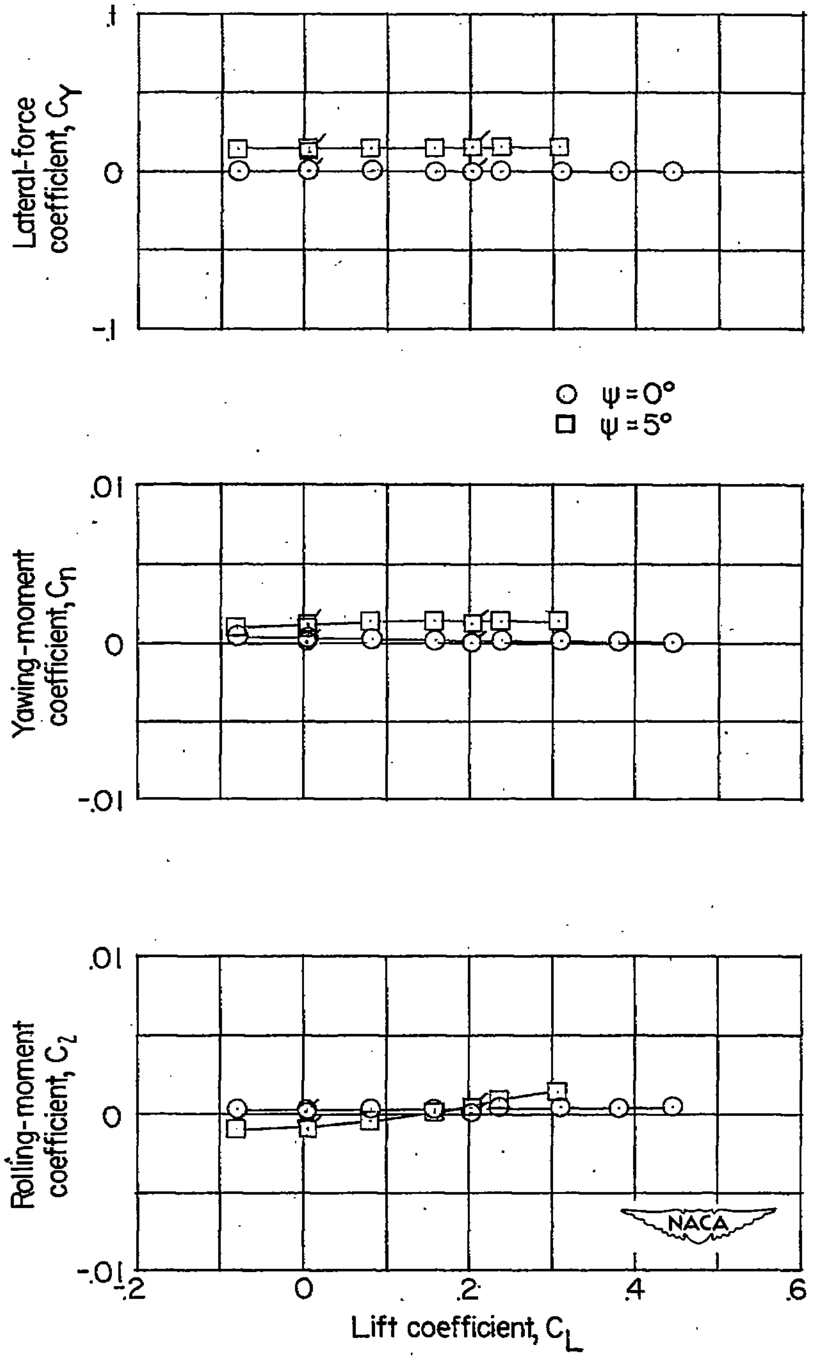

(e) $\Lambda = 47^{\circ}$; $\frac{t}{c} = 0.09$.

Figure 5.- Continued.

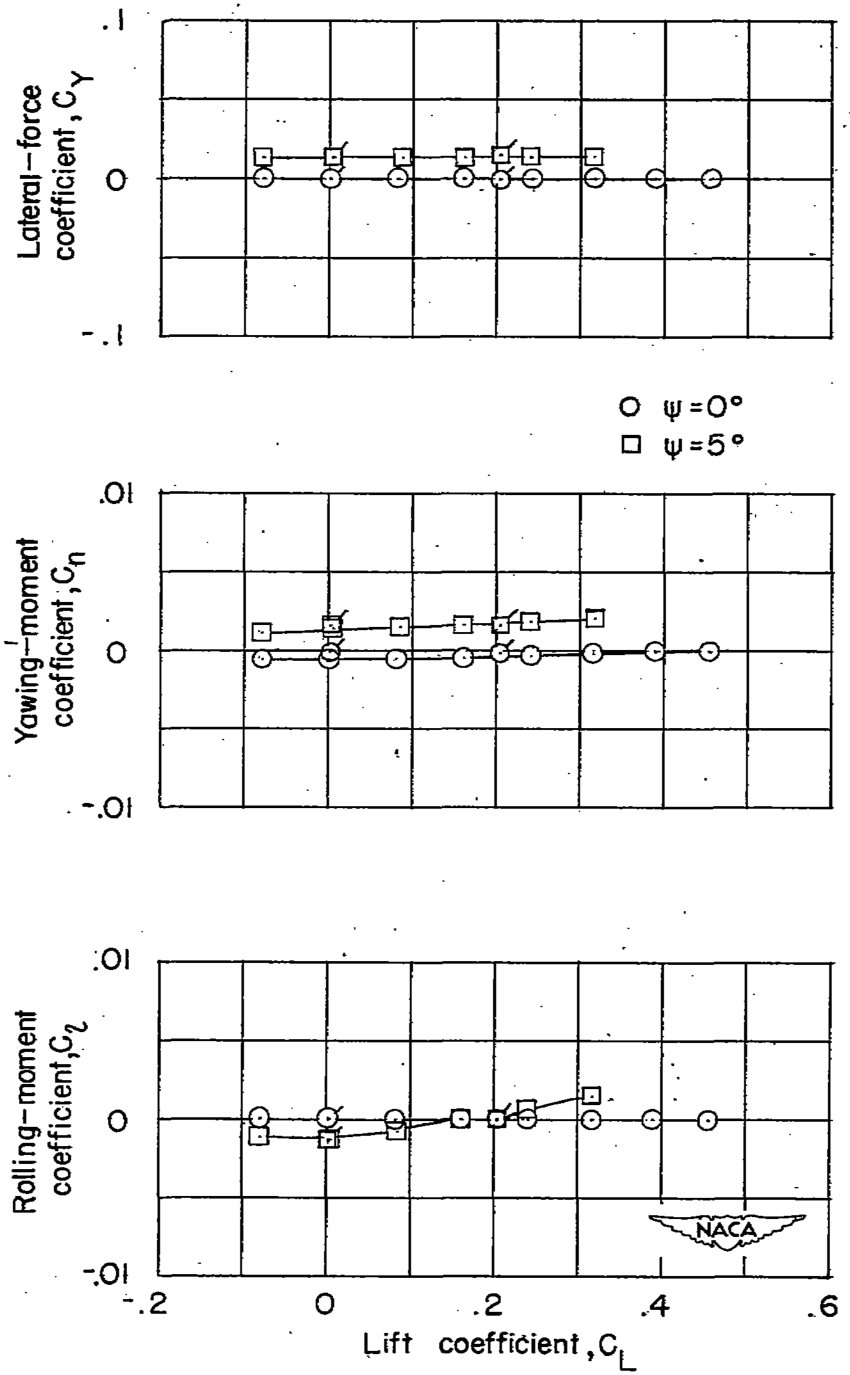

(f) $\Lambda = 47^\circ$; $\frac{t}{c} = 0.12$ to 0.06.

Figure 5.- Continued.

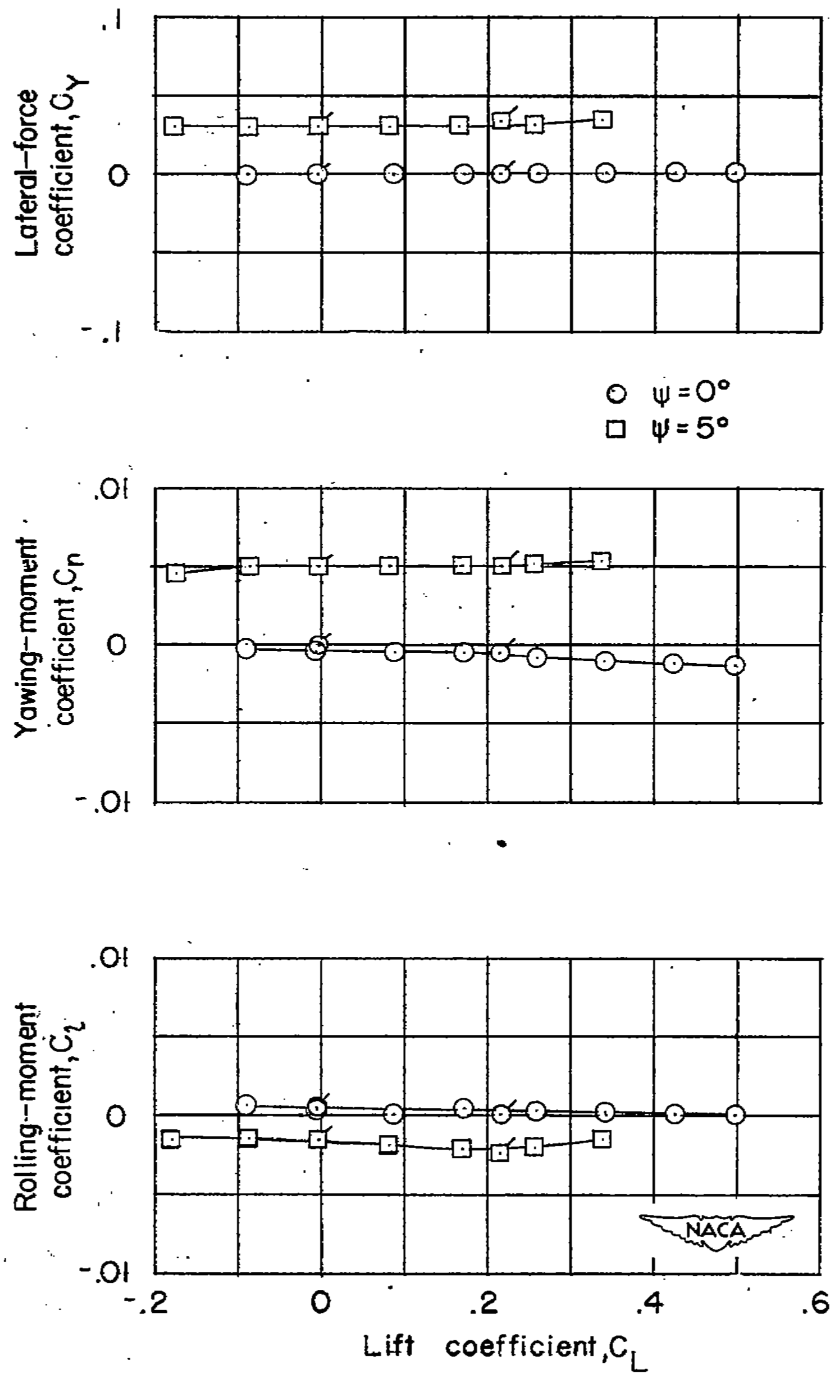

(g) $\Lambda = 47^\circ$; $\frac{t}{c} = 0.06$; nacelles on.

Figure 5.- Concluded.

[redacted]

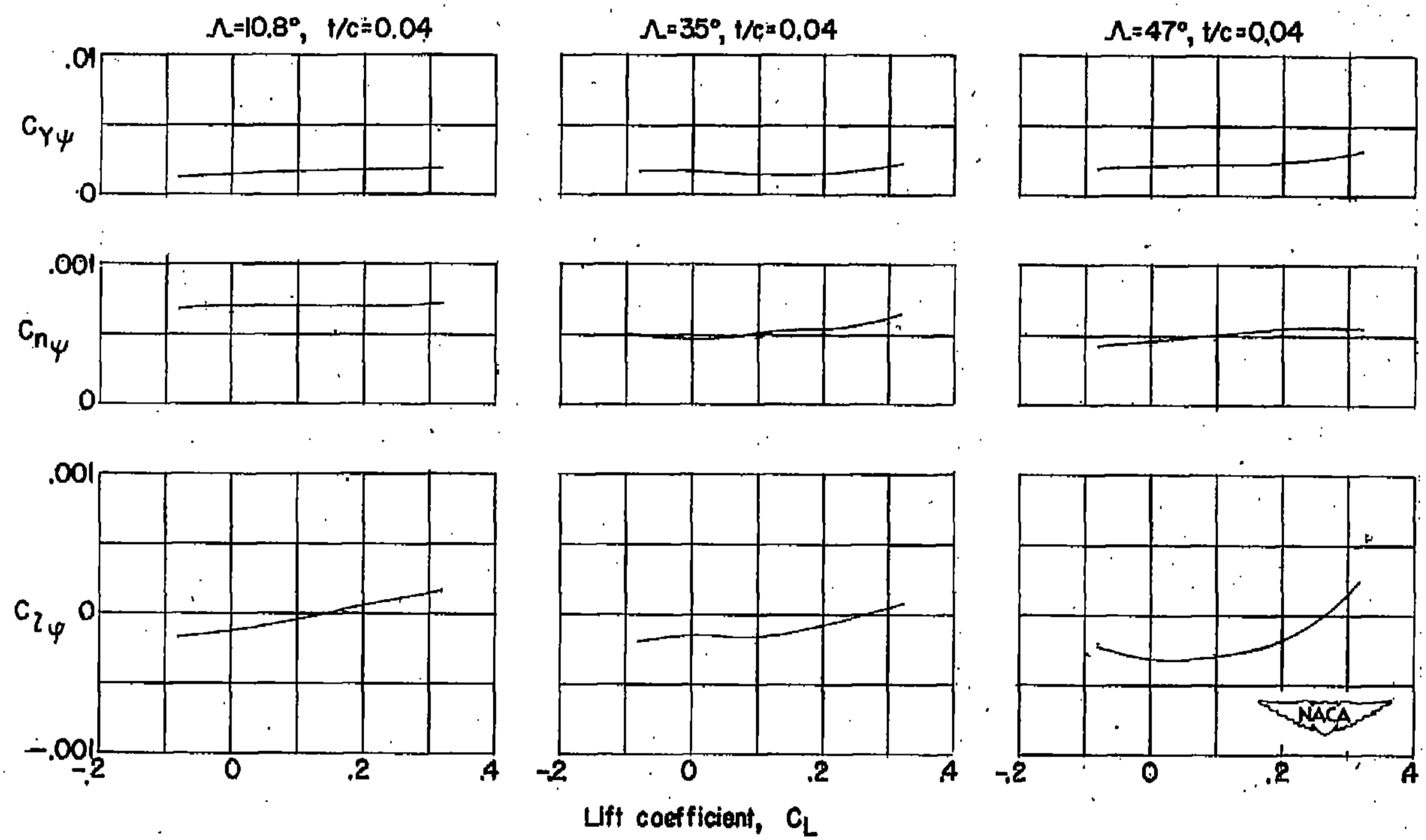

(a) Sweep series.

Figure 6.- Variation of the static lateral stability characteristics with lift coefficient for various wing-body combinations at $M = 2.01$.

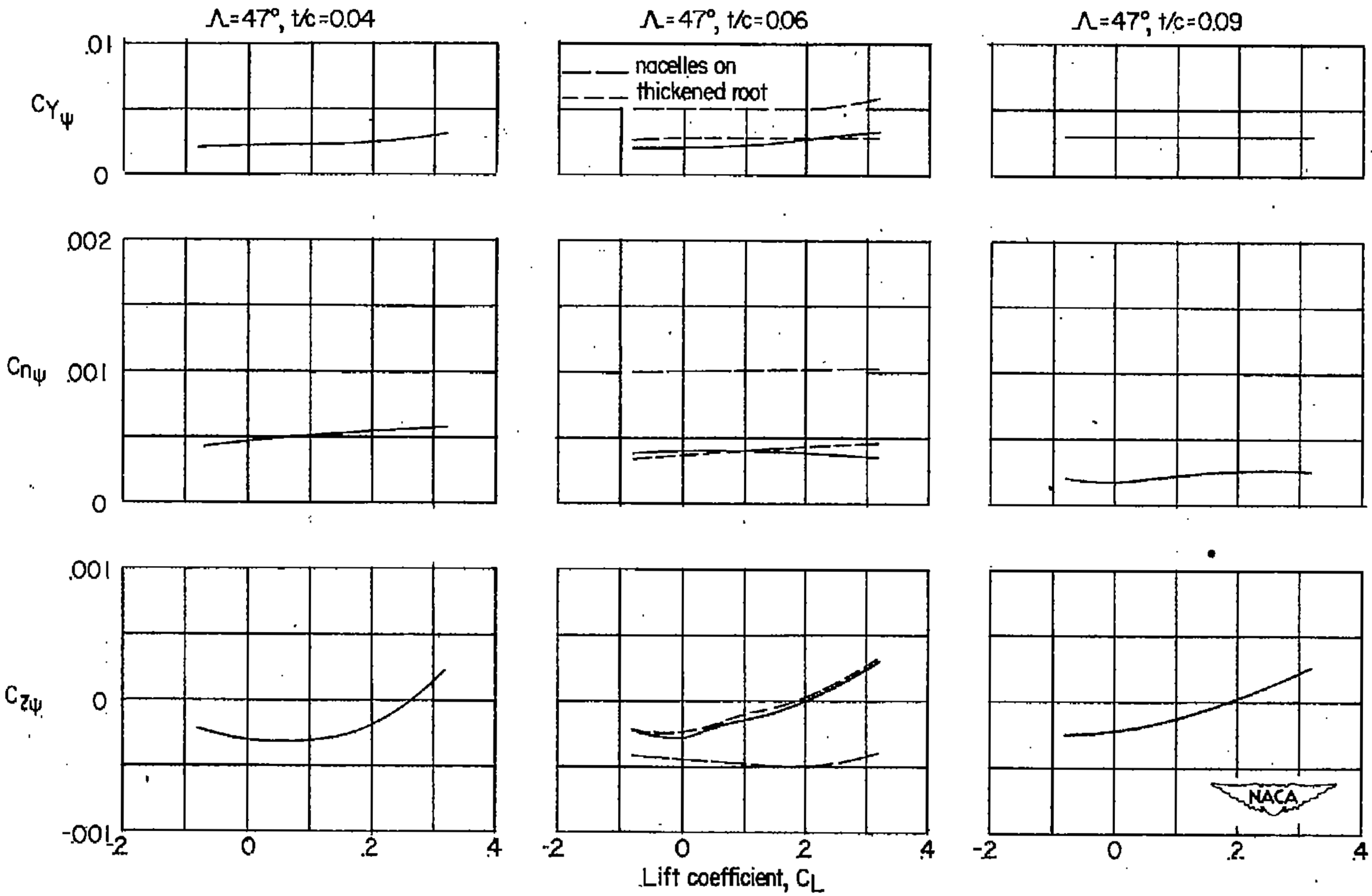

(b) Thickness series.

Figure 6.- Concluded.

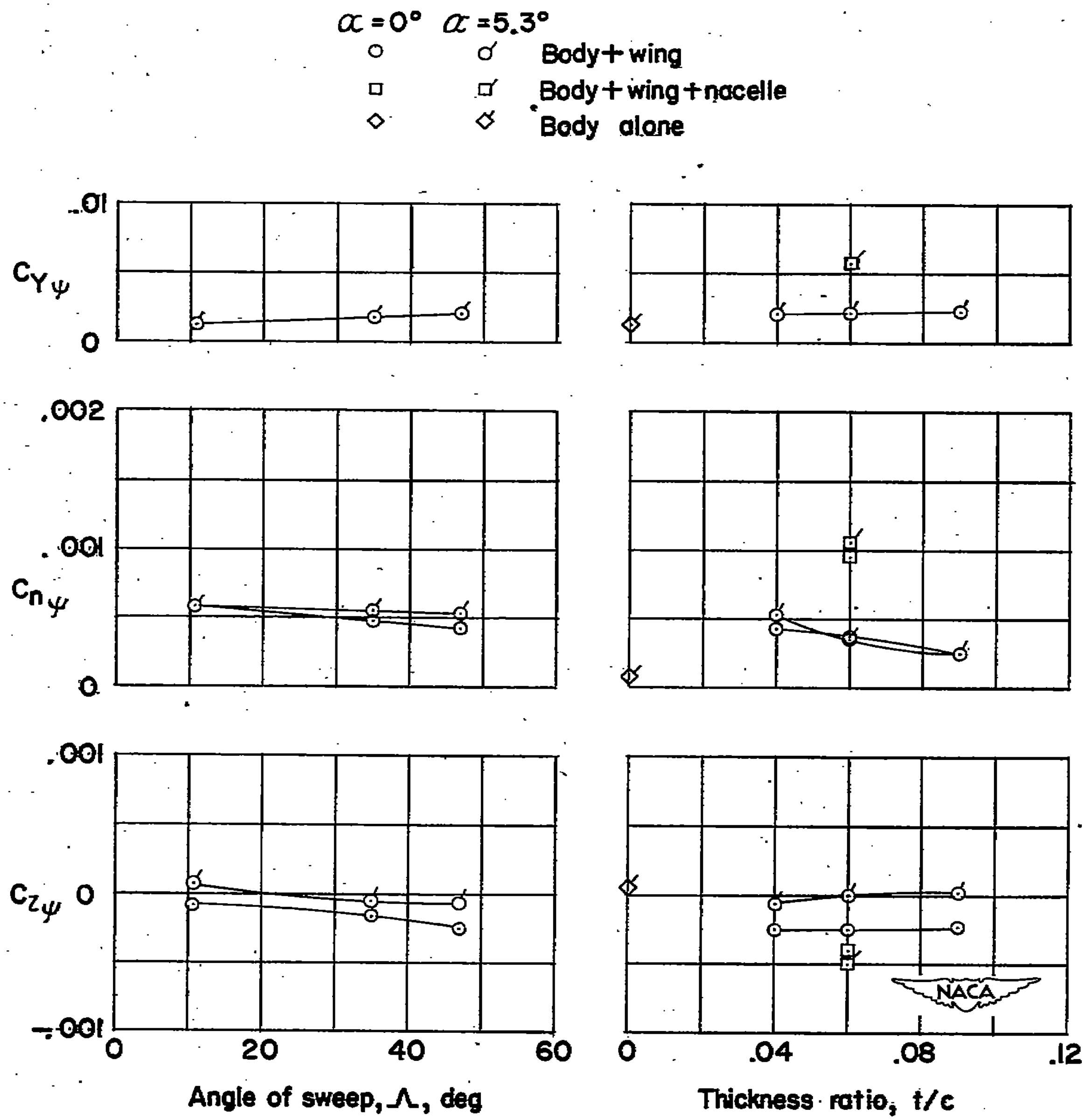

Figure 7.- Summary of the static lateral stability characteristics of various configurations at M = 2.01.

~~SECURITY~~ INFORMATION

[redacted]